DESIGN AND CHARACTERIZATION OF NONWOVEN FABRICS FOR GAS

DIFFUSION LAYER IN POLYMER ELECTROLYTE MEMBRANE

FUEL CELL

Except where reference is made to the work of others, the work described in this thesis is my own or was done in collaboration with my advisory committee.
This thesis does not include proprietary or classified information.

_____
Lale Isikel

Certificate of Approval:

_____	_____
Peter Schwartz Professor Polymer and Fiber Engineering	Sabit Adanur, Chair Professor Polymer and Fiber Engineering
_____	_____
Bruce J. Tatarchuk Professor Chemical Engineering	Carol Larson Warfield Professor Consumer Affairs

_____
George T. Flowers
Interim Dean
Graduate School

DESIGN AND CHARACTERIZATION OF NONWOVEN FABRICS FOR GAS DIFFUSION LAYER IN POLYMER ELECTROLYTE MEMBRANE FUEL CELL

Lale Isikel

A Thesis

Submitted to

the Graduate Faculty of

Auburn University

in Partial Fulfillment of the

Requirements for the

Degree of

Master of Science

Auburn, Alabama
May 10, 2007

DESIGN AND CHARACTERIZATION OF NONWOVEN FABRICS FOR GAS DIFFUSION LAYER IN POLYMER ELECTROLYTE MEMBRANE FUEL CELL

Lale Isikel

_____
Signature of Author

_____
Date of Graduation

VITA

Lale Isikel, daughter of Ahmet and Ayse Isikel, was born on September 17, 1981, in Bursa, Turkey. She attended the Ahmed Yesevi High School in Eskisehir, Turkey and graduated in June 1999. She entered Uludag University in September, 2000, and graduated with a Bachelor of Science degree in Textile Engineering in June 2004. In August, 2005, she entered the Graduate School at Auburn University.

THESIS ABSTRACT

DESIGN AND CHARACTERIZATION OF NONWOVEN FABRICS FOR GAS DIFFUSION LAYER IN POLYMER ELECTROLYTE MEMBRANE FUEL CELL

Lale Isikel

Master of Science, May 10, 2007
(B.S., Uludag University, 2004)

95 Typed Pages

Directed by Sabit Adanur

The aim of this research is to develop and evaluate materials for polymer electrolyte membrane fuel cells. Gas diffusion layer (GDL) is a part of membrane electrode assembly (MEA) that is the locomotive of polymer electrolyte membrane fuel cell (PEMFC). In this work, a PEMFC is built to study the MEA's behavior during operation. New gas diffusion layer structures are manufactured and their characterizations are done by compression-resistance test. The strength and resistance values of the new materials are comparable to those of the commercial materials tested.

ACKNOWLEDGEMENTS

First of all, I would like to express my gratitude to Dr. Sabit Adanur, my advisor, for introducing me to the field of fuel cell and providing me with the opportunity to pursue my master degree. Secondly, I thank my committee members, Dr. Peter Schwartz, Dr. Bruce Tatarchuk and Dr. Carol Warfield for their contribution. Also, special thanks to Dr. Faissal Abdel-hady for his help during the manufacturing of the fuel cell.

I wish to extend my thanks to all the former and present friends and colleagues for all the fun, joyous moments and creating a stimulating working atmosphere at the Polymer and Fiber Engineering in Auburn University. The financial support from the National Textile Center (NTC) is gratefully acknowledged.

I would also like to express my most sincere thanks to my parents, Ahmet, Ayse-Isikel, and my sister for always supporting me. Thank you for all the inspiration you have given me.

Style manual or journal used: The Harvard Journal Style

Computer software used: Microsoft Office 2003

TABLE OF CONTENTS

LIST OF FIGURES

LIST OF TABLES

CHAPTER I

INTRODUCTION

"I cannot but regard the experiment as an important one…"

William Grove writing to Michael Faraday, October 22, 1842

Although the fuel cell was invented in 1839 by William Grove, its commercial potential was not recognized until the 1960s.

A fuel cell, basically, is an electrochemical device which produces electricity directly from a fuel, and the by products of fuel cell are usually heat and water. In this aspect, fuel cells are important for the environment and human health. The National Energy Policy Act (NEPA) indicates that motor vehicles in the US still account for 78% of carbon dioxide emissions, 45% of nitrogen oxide emissions and 37% of volatile organic compounds. As a consequence, one in four Americans breathes unhealthy air. It is worse in the rest of the world [1]. The introduction of fuel cells into the transportation sector will increase fuel efficiency, decrease foreign oil dependency and become an important strategy to ease to climate change. The Department of Energy announced that as fuel cell vehicles begin to operate on fuels from natural gas or gasoline, green house emissions will be reduced by 50%.

Fuel cell consists of an anode at which oxidation of fuel (hydrogen) takes place and a cathode at which reduction of oxygen occurs. The anode and cathode reactions take

place on a common electrolyte. The electrolyte defines the key properties, such as operating temperature, of the fuel cell so that fuel cell technologies are named by their electrolyte. There are five distinct types of fuel cells; polymer electrolyte membrane fuel cell (PEMFC), alkaline fuel cell (AFC), phosphoric acid fuel cell (PAFC), molten carbonate fuel cell (MCFC) and solid oxide fuel cell (SOFC). Among them, PEMFC has the advantages of low operating temperatures, quick start up time and its corrosion free materials [2-3]. However, it should be noted that low temperatures require use of expensive catalysts and its high cost electrolyte-solid membrane- has high sensitivity to fuel impurities. Moreover, the challenges facing their technical and economic development include thermal and water management, low cost-durable membranes, and low Pt-catalyst loading electrode structures.

The objective of this study is to develop light, high conductive, porous and stable materials for PEMFC electrodes. In proton exchange membrane fuel cells, carbon paper and carbon cloth are used effectively as electrode backing material, which is also called gas diffusion layer (GDL). Gas diffusion layers serve as current collectors that allow ready access of fuel and oxidant to the anode and cathode catalyst surfaces. The requirements of an ideal gas diffusion layer include, maintaining high surface area to catalyst layer, diffusing the gas reactants effectively to the catalyst layers, having high electronic conductivity, having a surface enhanced for good electrical contact and having a proper hydrophobicity for membrane hydration and prevention of flooding. It is desirable for fuel cells to operate at a relatively high current density for the highest power output with small total system. Higher operating current density of fuel cell requires

higher flux of gas feed. This implies that ideal gas diffusion layers should be able to effectively diffuse reactant gases to the catalyst surfaces at a high rate

Although the fuel cell is not constrained by Carnot limitations, other sources of irreversibilities cause inefficiency, such as ohmic losses and mass transport losses. Thorough characterization of gas diffusion layers is necessary in determining the mass transport limitations.

In this work, a PEMFC is built to study the membrane electrode assembly's (MEA) behavior during operation. New gas diffusion layer structures are manufactured and characterized.

CHAPTER II

LITERATURE REVIEW

The following section is a brief review of the fundamental background subjects, including (i) electrochemistry of polymer electrolyte membrane fuel cell (PEMFC) and (ii) structure of polymer electrolyte membrane fuel cell

Electrochemistry of Polymer Electrolyte Membrane Fuel Cell

The basic principle of hydrogen fuel cell is defined by its inventor William Grove in 1839. “A fuel cell is an electrochemical ‘device’ that continuously converts chemical energy into electric energy (and some heat) for as long as fuel and oxidant are supplied”[4]. In reality, degradation, primarily corrosion, or malfunction of components limits the practical operating life of fuel cells.

The operation type of fuel cell also has similarities with engines and batteries in terms of electrochemical nature of the power generation process. But unlike thermal engines a fuel cell does not have the limits of Carnot efficiency, and unlike the batteries a fuel cell does not need recharging as long as fuel supplied from an external source. Fuel cell uses liquid or gaseous fuels such as methanol, hydrocarbons and hydrogen. The oxidant is usually gaseous oxygen. Anode and cathode are composed of gases often in contact with catalyst to promote the power generating reaction. Unlike batteries, anode and cathode are not consumed during the cell operation.

The schematic of a hydrogen-oxygen polymer electrolyte membrane fuel cell is illustrated in the Figure 2.1.

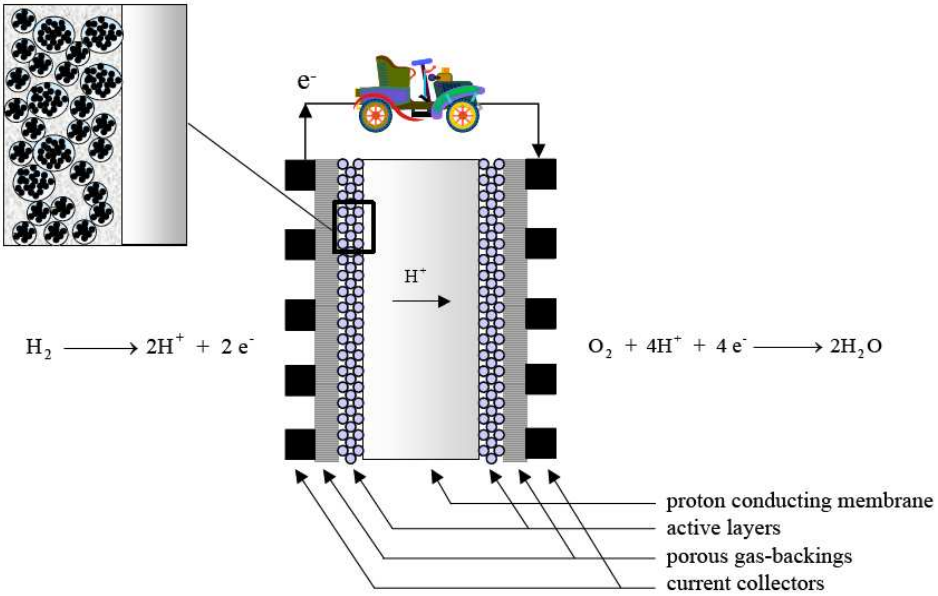

Figure 2.1 Schematic of the polymer electrolyte membrane fuel cell (PEMFC) principle [5]

During operation, at the anode of polymer electrolyte membrane fuel cell, the hydrogen gas ionizes and splits into its protons ($H^{+)}$ and electrons (e^-) by releasing energy, therefore the anodic reaction is

$$2H_2 \longrightarrow 4H^+ + 4e^- \qquad (2.1)$$

The protons pass through the electrolyte and reach cathode electrode. Continuously, the electrons travel through an external circuit to cathode electrode. At the cathode, oxygen reacts with electrons taken from the electrode, and H^+ ions from electrolyte, to form water. Cathode reaction is

$$O_2 + 4H^+ + 4e^- \rightarrow 2H_2O \qquad (2.2)$$

The overall reaction for hydrogen-oxygen polymer electrolyte membrane fuel cell is

$H_2 + O_2 \rightarrow 2H_2O$ (2.3)

Thermodynamics and Open Circuit Voltage

In a fuel cell, the energy of reactant and product is defined by "Gibbs free energy", that is the energy available to do external work that involves moving electrons round an external circuit, neglecting any work done by changes in pressure and/or volume. The difference between the Gibbs free energy of the products and the Gibbs free energy of reactants gives the energy released.

$$\Delta G_f = G_f of\ products - G_f of\ reactants$$

The most convenient consideration for these quantities is in their per mole form which is shown as Δg_f. In the basic operation of hydrogen-oxygen polymer electrolyte membrane fuel cell (PEMFC), the product is one mole of H_2O and the reactants are one mole of H_2 and half mole of O_2. Thus,

$$\Delta g_f = (g_f H_2O) - (g_f H_2) - 1/2(g_f O_2)$$

The Gibbs free energy of formation depends on temperature and state of the fluid (liquid or gas). Table 2.1 shows the Δg_f values at standard pressure (0.1 MPa) and different temperatures for the basic hydrogen fuel cell reaction (2.3)

Table 2.1 Δg_f for the reaction of H_2 + ½ O_2 $\rightarrow$ H_2O [6]

Form of water product	Temperature (◦C)	Δg_f (kJ mol^{-1})
Liquid	25	-237.2
Liquid	80	-228.2
Gas	80	-226.1
Gas	100	-225.2
Gas	200	-220.4
Gas	400	-210.3
Gas	600	-199.6
Gas	800	-188.6
Gas	1000	-177.4

When the values are negative, it means that energy is released. If there are no losses in the fuel cell, this Gibbs free energy will be all converted to electrical energy.

For the PEM fuel cell, two electrons pass around the external circuit for each water molecule produced. If the -e is the charge on one electron and N is Avogadro number, then the charge of flow,

$$2Ne = -2F \ coulombs$$

F is called Faraday constant which is equal to 96485.34 coulomb/mole.

If E is the voltage of the fuel cell, then the electrical work done moving this charge round the circuit is

$$Electrical\ work\ done = charge\ x\ voltage = -2FE\ \ joules$$

If the system is reversible (no losses), then the electrical work done is equal to the Gibbs free energy released Δg_f .

$$\Delta g_f = -2FE \;\therefore E = \frac{-\Delta g_f}{2F} \tag{2.4}$$

Equation 2.4 is defined as the electromotive force (EMF) or reversible open circuit voltage of the hydrogen polymer electrolyte membrane fuel cell.

For example, a hydrogen fuel cell operating at 25 °C has Δg_f = -237.2 kJ which is read from Table (2.1), therefore E is calculated as 1.23 V. This is the ideal reversible cell voltage at equilibrium at the standard pressure (0.1 MPa).Gibbs free energy changes with temperature. Equally important for Gibbs free energy are pressure and concentration. Therefore, Gibbs free energy equation can be rearranged for hydrogen fuel cell using thermodynamics as,

$$\Delta g_f = \Delta g^\circ_f - RTIn\frac{\left(P_{H_2}.P_{O_2}^{1/2}\right)}{\left(P_{H_2O}\right)} \tag{2.5}$$

Δg°_f is the change in molar Gibbs free energy of formation at standard pressure. In the equation R is ideal gas constant, 8.314472 $J\cdot K^{-1}\cdot mol^{-1}$ and T is temperature at Kelvin. To see how this equation affects electromotive force (EMF), it can be substitute into equation 2.4 to obtain

$$E = E^\circ + RTIn\frac{\left(P_{H_2}.P_{0_2}^{1/2}\right)}{\left(P_{H_2O}\right)} \tag{2.6}$$

where E° is the EMF at the standard pressure.

Equation (2.6) is known as Nerst equation and all the pressures in this equation are partial pressure that is the pressure when the gas is part of a mixture, because fuel hydrogen is usually has CO_2 impurity and oxygen is always part of air. Basically, Nerst equation describes the relation of differential partial pressure and differential potential.

For example, if a PEMFC is at 25°C where water vapor is neglected and it is assumed that anode hydrogen feed is pure and operating pressure is 34.47 kPa (5 psi,1.34 atm), then equation (2.6) yields to 1.23 V. This is the reversible open circuit voltage of the PEMFC at the given operating conditions. In practice the operating voltage is less 1.23 V because of irreversibilities will be explained later.

Operating Polymer Electrolyte Membrane Fuel Cell Voltage

When a fuel cell is put to operation, the operating voltage is less than the theoretical calculated voltage. The performance of a fuel cell is measured by its irreversibility characteristics that reduce the theoretical cell voltage.

Polarization

The departure of the cell potential from reversible (i.e. Nerstian) value upon passage of faradic current can be termed polarization [7]. Polarization is another term that is used instead of irreversibility. Current-potential curves obtained under steady-state conditions give the polarization curves of the fuel cell. It should be noted that in the steady-state conditions, it is assumed that the system variation by time is negligible. Figure 2.2 shows polarization curves of a typical hydrogen-air PEM fuel cell. Irreversibility of the fuel cell is categorized into four main areas; activation loses, fuel crossover and internal Currents, ohmic losses, mass transport and concentration losses.

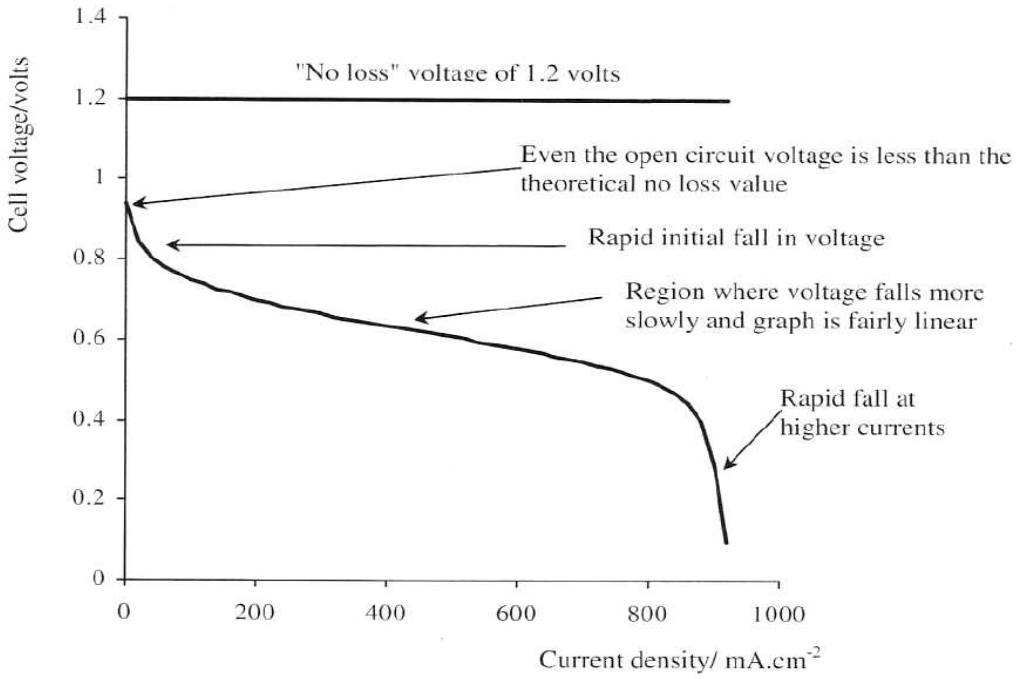

Figure 2.2 Polarization curve for a PEMFC [6]

Activation Losses

When hydrogen reacts and splits into electron and protons at the anode, energy is released; however, some energy must be supplied to get over the energy hill .This energy is called activation energy, which is the amount of energy that must be subtracted from Gibbs free energy of reaction for the reaction to occur. Activation losses are expressed by Tafel equation:

$$\Delta V_{act} = A\,In\left(\frac{i}{i_o}\right) \tag{2.7}$$

where A is the constant of Tafel equation, it can be shown for PEMFC that

$$A = \frac{RT}{2\alpha F} \tag{2.8}$$

where α is the charge transfer coefficient. Its value depends on the reaction involved and the material the electrode is made from, and it is in range of 0-10. i_o is called the

exchange current density. It might be visualized as follows: on the electrode surface when no current flows, there is no activity and reactions do not take place. However, the reactions are taking place all the time, and there is equilibrium. The current density on that equilibrium is called exchange current density, i_o. If this current density is high, and then the surface of the electrode is more active. The exchange current density is critical in controlling the performance of fuel cell electrode, especially gas diffusion layer. The appearance of T in equation (2.8) might give the impression that raising the temperature will increase the activation losses; but the effect of increase in i_o with temperature far outweighs any increase in A. As a summary, the smaller the i_o, the greater is the voltage drop.

Fuel Crossover and Internal Currents

The electrolyte of fuel cell is chosen according to its ion conductivity. Electrolyte is always support small amount of electron conduction that causes internal currents. In a practical fuel cell, some unused fuel will diffuse from anode through electrolyte to cathode where catalyst will react directly with the oxygen, producing no current from the cell. The crossing over of one hydrogen molecule from anode to cathode is defined as fuel crossover. This is essentially equal to two electrons crossing from anode to cathode internally, rather than external current. Therefore, these two effects, fuel cross over and internal current are assumed to be equal.

Working voltage of a cell will be less than the theoretical ‘no loss’ reversible voltage, but if no work is being done, theoretical voltage and cell working voltage should be the same. If it is supposed that a PEM fuel cell is in operation in air at ambient

pressure and at about 30 °C, and the fuel cell has only activation overvoltage losses on the cathode, then the voltage will be,

$$V = E - A\,In\frac{(i)}{(i_{\circ})} \tag{2.9}$$

For the given conditions, reasonable constants for equation (2.9) are chosen, E=1.2 V, A=0.06 V and i_o= 0.04 mA cm^{-2} .If the cell's current density is zero (at equilibrium), the cell open voltage will be 1.2V which can be calculated from equation (2.9). However, because of the internal current density, the cell current is not zero. For example if the current density is 1 $mAcm^{-2}$ then the open circuit voltage (V) would be 0.97V according to equation (2.9). It is over 0.2 V less than theoretical open circuit voltage (OCV).

Fuel crossover and internal current can not be measured by an ammeter inserted in the circuit. One is to measure the consumption of reactant gases. If a PEM fuel cell whose electrode area is 10 cm^2 might have an open circuit consumption of 0.004 $cm^3\,sec^{-1}$, at normal pressure and temperature, the volume of one mole any gas is 2.43 x $10^4 cm^3$ from Avogadro's law. Consequently, the gas usage is calculated as 1.646 x 10^{-7} s^{-1}.Hydrogen gas usage can be calculated for PEM fuel cell by

$$Gas\,usage = \frac{I}{2F}\,moles\,s^{-1} \tag{2.10}$$

I is the current that corresponds to losses and calculated as 31 mA from the formula (2.10). If the cell area is 10 cm^2, then the current density is 3.1 mA cm^{-2}. This current density gives the total current density including fuel crossover and internal current density. If i_n is representative total internal current density, then the equation (2.9) is refined to

$$V = E - A\frac{(i + i_n)}{(i_o)} \tag{2.11}$$

The internal current and fuel crossover losses are responsible for initial drop of the voltage-current density polarization curve which is shown in Figure 2.2; they have a very marked effect on the open circuit voltage of PEM fuel cell.

Ohmic Losses

Ohmic losses are due to resistance to the flow of electrons through the electrodes, collectors, contacts etc., basically it is the resistance to the flow of ions. In PEM fuel cell, the resistance is mostly caused by electrolyte, through the cell interconnections or bipolar plates. To reduce the disabilities in the connection, a compression pressure is applied to the layer of the cell during manufacturing process.

The current is responsible for the amount of voltage drop that is given by

$$V = I\ x\ R \tag{2.12}$$

Equation (2.12) can be expressed in as

$$V = ixr \tag{2.13}$$

where i $mA \cdot cm^{-2}$ is the current density and r $k\Omega\ cm^2$ is area-specific resistance, which is the resistance, corresponding to 1 cm^2 of the cell.

There are three ways of reducing the internal resistance [6]:1) Using highly conductive electrodes, 2) Good cell design in bipolar plates and current collectors, 3) Reducing the electrolyte thickness as much as possible

Mass transport and Concentration Losses

Mass transport is the process of supplying reactants and removing products. In the operation, there are two phase transport in PEM fuel cell: i) gas phase transport which is the form of reactants ii) Liquid phase transport which is the form of products (i.e., water)

Poor mass transport can be causes by a change in the concentration of reactant and product within the catalyst layer .The losses in the reversible open circuit voltage are called mass transport losses or concentration losses.

At the cathode of an air/hydrogen fuel cell, as the oxygen is extracted from the air, there will be a slight reduction in the concentration of oxygen during the cell operation. The extent of this change in the concentration will depend on the current being drawn from fuel cell and the physical factors relating how well the air around the cell, and how quick the oxygen can be replenished. Moreover, at the anode, while the hydrogen is being supplied, there will be a slight reduction in the pressure due to the fact that there will be flow of hydrogen down the supply ducts and tubes, and this flow will result in a pressure drop due to their fluid resistance.

In both cases, reduction in concentration and in partial pressure of reactant and product will cause performance drop and voltage losses.

Voltage drop can be calculated by

$$E = E^{o} + \frac{RT}{2F\ In\left(\frac{P_{O_2}^{1/2}}{P_{H_2O}}\right)} + \frac{RT}{2F\ In\left(P_{H_2}\right)} \qquad (2.14)$$

So if the hydrogen partial pressure change is responsible for concentration losses, and its partial pressure changes from P_1 to P_2, with P_{O_2} and P_{H_2O} remain unchanged, concentration losses can be formulated by

$$\Delta V = \frac{RT}{2F\ In\frac{P_1}{P_2}} \tag{2.15}$$

Limiting current density, i_L, in the catalyst layer, is the maximum current density that can be used to obtain ideal electrode reaction without polarization. It is termed as the maximum current density where the current density cannot rise above during operation because the fuel cannot be supplied at a greater rate. If the pressure P_1 is the pressure when current density is zero, and P_2 is the pressure at any current density, then it is formulated by

$$P_2 = P_1\left(1-\frac{i}{i_L}\right)$$

Then equation (2.15) can be refined as

$$\Delta V_{Trans} = \frac{-RT}{2F\ In\left(1-\frac{i}{i_L}\right)} \tag{2.16}$$

It should be noted that the pressure falls linearly down to zero at the limiting current density, i_L.

However, it is a theoretical approach and can not comprise the change in the oxygen partial pressure especially in the case of cell supplied with the air rather than pure

oxygen- which is the vast majority. There are also problems when hydrogen is supplied as a gas mixture of carbon dioxide for the fuel. No account is taken for the production and removal of reaction products, such as water and for the built-up nitrogen in the air system.

Because of these weaknesses, Kim et al., [8] and Chahine et al., [9] introduced an approach that is empirical and yields an equation that fits the results very well and shown in equation

$$\Delta V_{Trans} = m \exp(ni) \tag{2.17}$$

The value of m will be typically about $3x10^{-5}$ V and n about $8x10^{-3}\,cm^2/mA$.

Mass transport losses can be decreased by; 1) pure oxygen feeding to the cathode instead of air, 2) preventing the hydrogen pressure reduction, 3) an effective supplying system, 4) increasing hydrogen purity

Moreover as design strategies; i) to increase the limiting current density gas diffusion layer thickness should be reduced, ii) Flow field plate should be improved for even distribution of reactant and product which will prevent diffusive losses iii) The electrode structure and operating conditions should be optimized for ensuring a high value of diffusion coefficient (D).

Combining the Total Voltage Losses

All voltage losses can be combined as:

$$V = E - \Delta V_{ohm} - \Delta V_{act} - \Delta V_{trans}$$

$$V = E - ir - A\,In\left(\frac{i + i_n}{i_o}\right) + m \exp(ni) \tag{2.18}$$

This equation is simplified in a useful way in practice. In many fuel cells including PEMFC, the crossover current i_n is very small. Although it is useful to explain the initial drop in the polarization curve, it can be negligible since it has little impact on operating voltage losses. Therefore, the activation overvoltage can be written as

$$\Delta V_{act} = A\,In\frac{i}{i_o} = A\,In(i) - AIn(i_0) \tag{2.19}$$

It is indicated that i_o (exchange current density) is always smaller than the operating current density; thus it can be negligible, and the equation will be reduced to

$$\Delta V_{act} = A\,In(i)$$

As a result the operating voltage formula can be redefined as

$$V = E - ir - A\,In(i) + m\exp(ni) \tag{2.20}$$

Equation (2.20) is simple and it gives an excellent fit with the real result of fuel cell.

Proton Electrolyte Membrane Fuel Cell

Polymer electrolyte or proton exchange membrane fuel cells (PEMFCs) have a solid proton exchange membrane as its electrolyte. The proton exchange membrane fuel cell, PEMFC, takes its name from that special ionomer membrane.

All the key parts of PEMFC which are cathode, anode and solid membrane, are combined in a very compact and thin unit. This unit is called membrane-electrode assembly, MEA. The MEA is typically located between a pair of current collector plates with machined flow fields plates for distributing fuel and oxidant to the anode and cathode.

Membrane- Electrode Assembly (MEA)

In PEMFCs, the anode-electrolyte-cathode assembly (membrane electrode assembly or MEA) are connected in series with bipolar plates. Since the solid electrolyte membrane can not diffuse into the porous electrode structures, the electrolyte-gas interface has two-dimension, and there might be parts that do not adhere to each-other. In order to produce a high interface area, a special bonding procedure is required to prepare the membrane and electrode assemblies.

To provide sufficient catalytic activity, platinum or platinum alloy is applied into the membrane electrode assembly. Catalyst layer can be applied directly to the membrane by many different methods. In one method, metallic catalyst layer is formed on the solid membrane electrolyte; in another method, catalyst layer is applied to the gas diffusion layer followed by membrane addition.

The chemical reactions take place on MEA. There are three main ways of dealing with the slow reaction rates [6];

- The use of catalysts
- Raising the temperature
- Increasing the electrode area

The first two can be applied to any chemical reaction; however the third one is important to the fuel cells. Electrode in the fuel cell consists of three main parts: 1.Catalyst; 2. Thin electrode layer; 3. Gas diffusion layer (Figure 2.3).

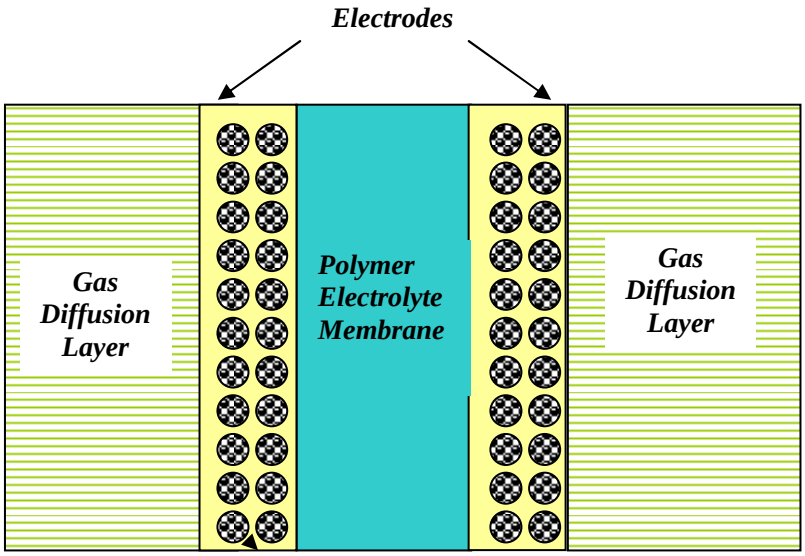

Figure 2.3 Schematic of five layers membrane electrolyte assembly

Polymer Membrane

Polymer electrolyte membranes have the ability of ion-exchange. In ion exchange membranes, charged groups are attached to polymer backbone of the membrane material. These fixed charge groups partially or completely exclude ions of the same charge from the membrane. This means that anionic membrane with fixed positive groups excludes positive ions but it is freely permeable to negatively charged ions. Similarly, a cation membrane with fixed negative groups excludes negative ions but it is freely permeable to positively charged ions. Cation exchange membranes were originally developed for chlor-alkali industry by DuPont (Figure 2.4).

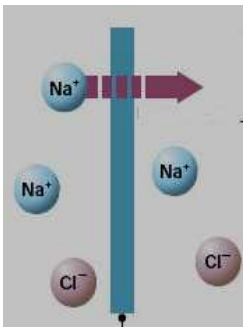

Figure 2.4 Schematic of cation-exchange membrane mechanism

Polymer electrolyte membrane in a fuel cell is a cation-exchange membrane and can have mobile H^+ ions to carry the protons from anode side to the cathode side of the fuel cell. Different companies have been producing different polymer electrolyte membranes with their proprietary techniques. However, a common theme is the use of sulphonated fluoro-polymers, usually fluoroethylene. The most well known and well established of these is Nafion® (by DuPont) which has been developed since the 1960s and was first used by GE in 1966 for NASA's space mission work [10].

The starting point of the electrolyte membranes is basic, man-made polymer-polyethylene. Then, polyethylene is modified by replacing the hydrogen (H) atoms with the fluorine (F) atoms; this process is called perfluoronation. The monomer is called tetrafluoroethylene; the modified polymer, polytetrafluoroethylene, or PTFE is also sold as TEFLON®, the registered trade mark by DuPont. Strong bonds between the fluorine and carbon make PTFE durable and resistant to the chemical attacks and provide waterproof properties. (The same property gives it a host of uses in outdoor clothing and footwear.)

However, to have an ion-exchange electrolyte, a further step is needed. The basic PTFE polymer is sulphonated – a side chain is added, ending with sulphonic acid HSO_3.

A possible side chain structure is shown in Figure 2.5; the details vary for different type of Nafion® and with different manufacturing practices of membranes.

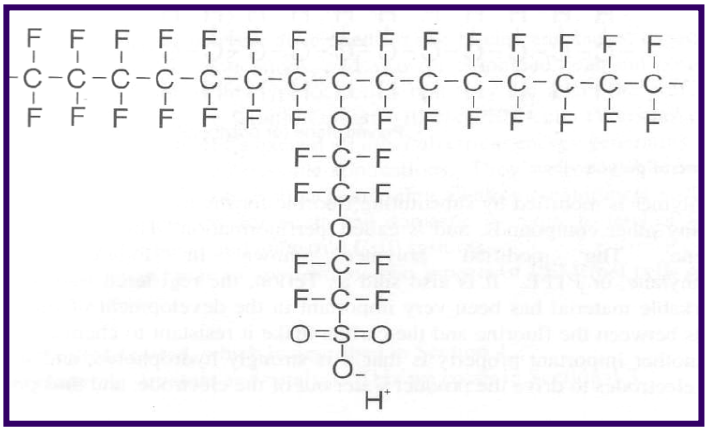

Figure 2.5 Example structure of perfuorosulphonic acid PTFE copolymer [6]

The HSO_3 group is ionically bonded, and side chain has the SO_3^- ion. As a result of the presence of these SO_3^- ions and H^+ ions from the electrode, there is a mutual attraction between the + and – ions from each molecule. The result is that the side chains tend to cluster within the overall structure of the membrane. Another key property of the sulphonated membranes is that the sulphonated end groups (HSO_3) are highly hydrophobic. The hydrophobic regions around the clusters of sulphonated side chains can absorb large quantities of water, increasing the dry weight of material by up to 50% [6]. Within these hydrated regions, the H^+ ions are relatively weakly attracted to the SO_3^- group and are able to move. This creates a dilute acid region within the though and are hydrophobic regions. This "micro-phase separated morphology" is shown in Figure 2.6. Although the hydrated regions are somewhat separate, it is still possible for the H^+ ions to move through the supporting long molecule structure. Thus, it is easy to see that for this to happen; the hydrated regions must be as large as possible. In well hydrated electrolyte,

there will be about 20 water molecules for each SO_3^- side chain [6]. As the water content falls, the conductivity falls in a more linear fashion.

Nafion® has high mechanical strength and resistance to chemical attacks, such that it can be made into very thin films, as low as 50 μm. If it is well hydrated which means H^+ ions can move fairly freely within the material, it will provide good ion conductivity. In a well humidified Nafion® membrane, conductivity can be as high as 0.2 S/cm at PEMFC operating temperature; this conductivity translates to the cell resistance as low as 0.05 Ω cm^2 for a 100 μm thick membrane with a voltage loss of only 50 mV at 1 A/cm^2 [11].

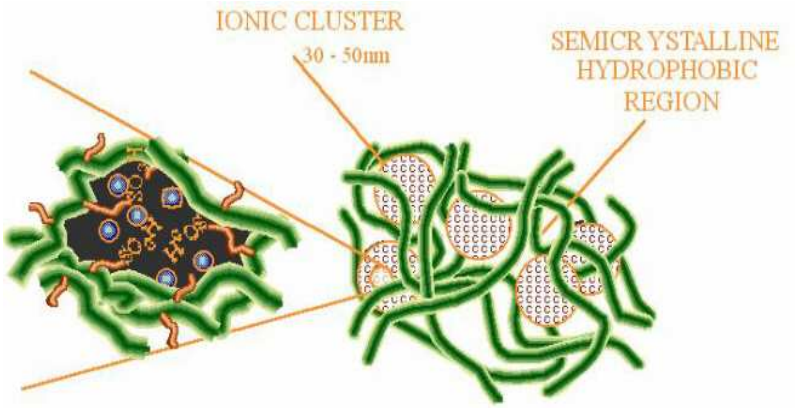

Figure 2.6 The schematic of Nafion®-type membrane materials [12]

Given these advantages, perfluoro-sulfonic acid (PFSA) membrane suffers from several drawbacks. Its low-proton conductivity at low relative humidity limits the operation temperature to about 80 ˚C. It has poor mechanical properties above 130 ˚C. High methanol crossover (-CO) causes inefficiencies on the catalyst [16]. Electro-osmotic drag, each proton (H^+) crosses through membrane and drags at least five water molecules. Moreover the membrane has high cost, currently averaging US$ 25kW, and humidifying of the membrane to have high ion conductivity adds extensive supporting

external equipments [17]. Additional disadvantages were reported like arising toxic and corrosive gases at the temperatures above 150 ˚C. Decomposition gases could be a concern during manufacturing emergencies or vehicle accident. Fuel cell recycling also presents challenges.

Catalyst Layer

Platinum-based catalysts are the most suitable catalysts for both anode and cathode in PEMFC. Since platinum (Pt) catalyst is still a major cost factor in fuel cells, instead of pure platinum, platinum-based catalysts are used to reduce the cost. The platinum-based catalyst is formed into very small particles and deposited onto the finely grounded carbon powders as shown in Figure 2.7. Carbon-based powder XC72 (® Cabot) is widely used.

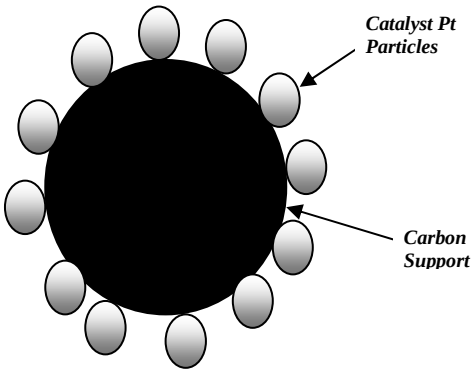

Figure 2.7 Idealized structure of carbon-supported catalyst

To counter the problem of CO poisoning on the catalyst layer, there are at least seven Pt-based catalysts that give performance equal or similar to that given by Pt/C with pure hydrogen cell: Pt-Ru/C, Pt-Mo/C, Pt-W/C, Pt-Ru-Mo/C, Pt-Ru-W/C, Pt-Ru-Al_4, and Pt-Re-(MgH_2).

Gas Diffusion Layer

Gas diffusion layers (GDLs) in polymer electrolyte membrane fuel cell are usually made of a porous carbon paper or cloth, typically in thickness of 0.30-1.00 mm. Gas diffusion layers are adjacent to the bipolar plates on the anode side and cathode side.

Mainly, GDL should provide even reactant gases (both hydrogen and oxygen) distribution from flow field channels to catalyst layer including in-plane gas distribution from flow fields to adjacent land area. Reactant gas, hydrogen, produces electrons on the catalyst layer. Firstly, GDL has to have electronic conductivity to carry electrons towards the electron collectors. GDL should provide through plane electronic conductivity, perpendicular to electron collector and in-plane electronic conductivity to regions adjacent to channels.

Secondly, gas diffusion layer provides passage for removal of product water from catalyst-layer area to flow-field channels including in-plane permeability of product water from regions to adjacent lands. The heat produced during oxidation in anode is removed from membrane electrolyte assembly (MEA) to the coolant channels of fuel cell by GDL.

Thirdly, GDL provides mechanical support to the thin, brittle membrane and catalyst layer against compressive forces which are applied during the assembly of fuel cell [18-19].

The functions, which are to supply reactants to the catalyst layer, to collect the current, to remove heat and product water from the MEA and to provide mechanical support to the catalyst layer and membrane, require different structural and chemical properties. While air and water permabilities increase with porosity, electrical and

thermal conductivities decrease with porosity [20]. To better understanding structure of GDL structural parameters will be explain individually.

Imperative Properties of Gas Diffusion Layers

Porosity

Porosity of GDL layer has a large effect on the PEM fuel cell performance. The key task of gas diffusion layer is the effective transportation of reactants to catalyst layer.

One problem which causes inefficiency in the PEM fuel cell is unexposed areas which are also termed land areas (the areas stays under flow field plate's lands). Unexposed areas (as I in Figure 2.8), do not connect with the reactants directly; the reactants are distributed by GDL to these regions efficiently. Otherwise, electron conductivity might be decreased due to unused catalysts in unexposed land areas.

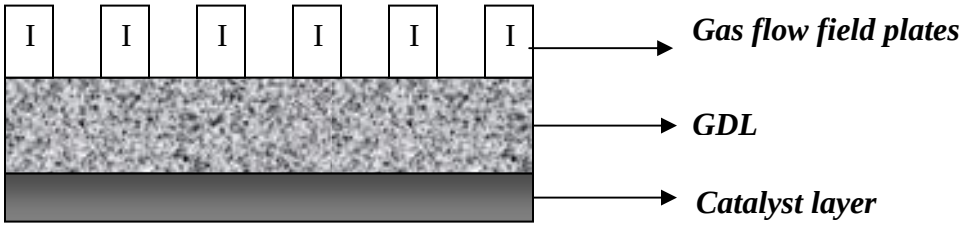

Figure 2.8 Schematic of cross-section of gas diffusion layer and gas flow channels

In the process, porosity is affected by compression of the stack and water production at the cathode. These factors change the porosity of the gas diffusion layers. Roshandel et.al. [21] investigated the effect of porosity of the anode and cathode gas diffusion layers. First, it was assumed that porosity distribution, reactant concentration in the GDL/membrane interface and electrical current density are all uniforms. The average of electrical density was measured (~ 0.61A/cm^2). In the second step of the study, porosity was considered as a function of compression pressure; due to compression,

porosity decreases especially under the landing area. Reduction in porosity results in more uniformity in the gas diffusion layers. Some catalyst particles, especially under landing area, remain unused and the average electrical current density reduces to 0.47A/cm2 (~23% less). The result of this study is that the compression pressure can lead to 32% decrease in porosity and up to 10% decrease in reactant transportation in GDL. Lee at al. [22] stated that electrical resistance decreases quickly with the stress applied on GDL.

Thickness

The thickness of gas diffusion layer has effect on reactants gas transport to the catalyst layer. Commercial GDL layers are available in various thicknesses. Thinner GDLs might be beneficial to transport the reactant gases which are oxygen and hydrogen. Thick GDLs may be desirable to obtain more flexibility which is necessary for fuel cell to handle the compression, to establish maximum contact between cell components and to improve the connected areas. Gas diffusion layers can support the ionomer membrane during the operation due to swollen membrane.

In the study of Sun et al. [23], results indicated that the average current density is not affected significantly as GDL thickness is reduced from 0.35 mm to 0.15mm. Also, this study showed that the effect of GDL thickness on current density depends on both oxygen and electron transport.

In summary, gas diffusion layer should be thick and flexible enough to handle mechanical compression and to support the electrolyte membrane. On the other hand, it should be thin enough to provide optimum connection at the interface between flow field plates and catalyst layer, for effective transport of reactant gases.

Hydrophobicity

Efficient water management is a key factor in polymer electrolyte membrane fuel cells, due to sufficient water content need in the polymer membrane electrolyte. Previously, it was indicated that proton conductivity is directly proportional to water content. However, insufficient humidification of the membrane leads the elevated cell resistance by blocking the pores in the gas diffusion layer. A balance is needed.

To better understand the water management, several complications has to be understood well. One is that during the operation of the cell, H^+ ions moving from anode side to cathode side through the polymer electrolyte membrane pull water between one and five water molecules that is called electro-osmotic drag. Consequently, even if the cathode side is well hydrated, the anode side of the electrolyte can be dried out. Another complication may be due to temperature of the reactants. For example, during the cell start-up, when a warm, humid reformatted stream is fed to a cool cell, it might result in significant water condensation; or at temperatures around 60 $^{\circ}$C, the cathode air dries the cathode out faster than the water produced in the cathode side. While lack of humidification causes these problems, excess water causes flooding in the fuel cell and obstructing reactant diffusion to the reactant sites, resulting in high mass transfer over potential. Consequently optimized GDLs reduce the need for external water management devices, and auxiliary power consumption. Especially, in small applications, the number of auxiliary devices should be minimized due to the size and complexity limitations[24].

PEMFC Gas Diffusion Layer Materials

Carbon Fiber Based Gas Diffusion Layer

Carbon fibers used in gas diffusion layers are based on polyacrylonitrile, (PAN) precursor whose density is approximately 1.17 g/cm^3 and with a molecular structure comprised of oriented, long chain molecules. Process steps to produce carbon fiber from PAN are spinning, stabilization, carbonization and finishing [25]. A single carbon filament is a long cylinder with a diameter of approximately 7 μm and packed like ribbon-like crystallites which are parallel to the fiber axis. Each crystal layer is made of carbon atoms arranged like a wire in a hexagonal structure, characteristic of graphite. Strong covalent C-C bonds within the layer plane give the potential for high strength and stiffness. Weak van der Waals bonding between the layers gives poor shear resistance; but on the other hand it has beneficial effects for thermal and electrical conductivity. Loose electrons and thermal energy use the inter-plane space as a corridor to travel. Typically, larger and more oriented graphene planes results in higher thermal and electrical conductivity. This can be accomplished by stretching the fiber after spinning and during stabilization steps in the manufacturing process. Further, in the stabilization step, PAN fibers are treated with heat at a temperature range of 200 to 300°C in an oxygen containing atmosphere to have further orientation and then crosslink the molecules for carbonization process. In this way, they can survive in high temperatures.

The most promising media in PEMFCs are PAN-fiber-based products, such as non-woven papers and woven fabrics due to their high porosity (>70%) and good electrical conductivity. As shown in Figure 2.9, carbon-fiber paper is bound by webbing, mostly

using carbonized thermoset resin, while carbon cloth needs no binder due to its woven structure

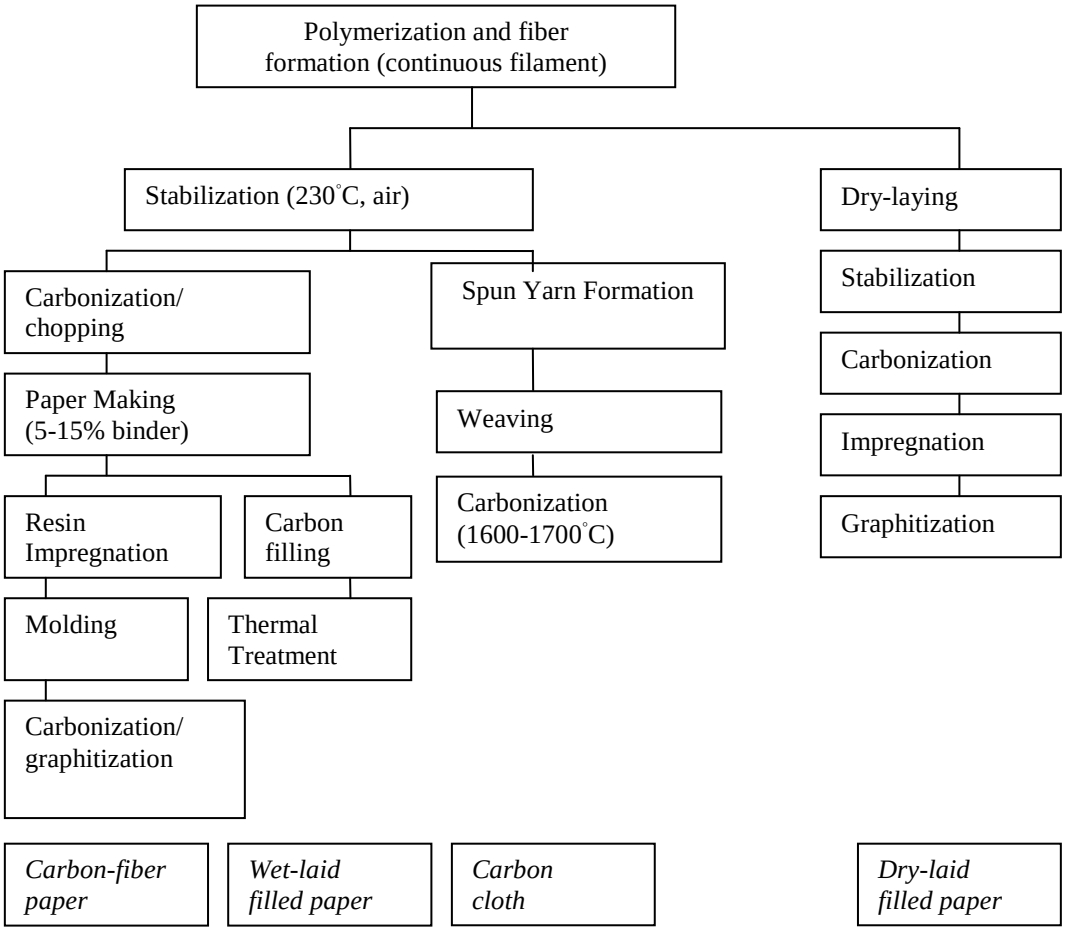

Figure 2.9 Processing routes for producing PEFC diffusion-media materials using PAN-based carbon fibers [25]

The nonwoven substrates that are used as gas diffusion layer are mostly wet-laid carbon fiber papers. In the traditional carbon paper wet-laid method chopped carbon fibers are dispersed in water with binders, commonly, with PVA (0.001 % by weight of the fiber). Dispersion is then fed to a ‘headbox’ which drops the dispersion onto a

rotating porous drum or wire screen with a vacuum dryer to remove the water [4]. The wet web is dried in an oven or hot, large diameter (1-2 m) rotating drums. Then, the material is rolled up at the end of drying procedure. The typical binder content is 5-15 % by weight of fiber, the weight is 45-70 g/m^2 and thickness is 0.20-0.27 mm. Carbon-fiber web is then sent to resin impregnation, which allows the paper to be molded to a desired thickness and density. Phenolic resins are typically used due to their high carbon yield (50 % of initial weight). In resin impregnation, methanol based solvents can be used, then heated to 150 $^{\circ}$C in air for solvent evaporation and resin oligomerization. At 175 $^{\circ}$C under 400-550 kPa, resin impregnated papers are molded; silicon coated separator papers can be used i molding step. Molding is done at a certain pressure or desired density or desired thickness. Finally, carbon-fiber paper has carbonization/graphitization step. Inert-gas heat treatment affects the weight, thickness and resistivity of a carbon-fiber/phenolic non-woven that has been molded and cured. During heat treatment the material looses 30-40% of its initial weight. Around 1000 $^{\circ}$C, most of the properties are changed due to phenolic resin degradation. Carbon-fiber web is usually heat treated till 1300 $^{\circ}$C, and after till 2200-2400 $^{\circ}$C, there is a dramatically decrease in resistivity.. The finished product is available in thickness ranging from 0.15 to 0.30 mm.

Another product from the wet laying process is called wet-laid filled paper. The difference from the traditional carbon-paper making method is that a carbon or graphite powder can be added and bond with PTFE. After wet-laying step, resin impregnation and molding steps can be skipped and carbon or graphite powder is mixed with polymer binder PTFE or PVDF (polyvinylidene fluoride). Then, this non-catalyst paste is applied on carbon-fiber wet-laid nonwoven media. Coating of non-catalyst paste is mostly done

by doctor blade method. Screen printing, spraying and rod coating are also used. Companies developing products using this approach are Lydall (US) and Technical Fibre Products (UK).

Carbon Fiber Cloth Gas Diffusion Layer

The carbon fabrics used as gas diffusion layer are either woven or knitted from spun PAN yarns. Rather than being held by resin, their woven structures provides mechanical strength needed.

In the process, a large stabilized acrylic tow, as precursor is produced first. Typically, the “worsted process” [19] may be used. It consists of running the precursor through a stretch-breaking machine which pulls the tow between nip and rolls at faster rate than it releases it. The result is randomized breaking of all the filaments which keep the fiber lengths between 1.3-5.0 cm The material then runs through equipment that blends and homogenizes it while increasing the effective yield (in length per kilogram) of the yarn. Then, the yarn is sent to spinning where twist or turns are imparted to yarn to hold it together. Twisted yarn is then plied; usually two ply, and wound on a bobbin for weaving.

In weaving, two common structures are used; one is plain weave and satin weave. In a plain weave, the fill (cross machine direction) goes over and under every warp yarn (machine direction), resulting in a very tight fabric. In an eight harness satin weave, the fill yarn can go over seven warp yarns before going under one warp yarn and then repeating such that the fabric is looser than plain weave fabric. Plain weave is preferred in gas diffusion layer because of its dimensional stability. The woven rolls of continuous

fabric need carbonization usually under 1600 °C. Producers of carbon cloth are Ballard Material Systems (Textron, US) and Zoltex (US) [4].

Dry-laid Gas Diffusion Layers

Pre-stabilized PAN fibers are dry laid into a thin fiber fleece mat through a carding-combing process. This mat then is bound by hydroentangling, a process in which a curtain of very fine 80-150 μm diameter water jets with spacing of 15-50 jets cm^{-1} pulsed onto the moving mat. This causes some fibers to orient through-plane direction and produces mechanically bonded nonwoven fabric. The PAN nonwoven mat is then oxidatively stabilized followed by carbonization to 1000-1500 °C [26]. The material can be optionally filled with carbon powder with addition of resin binder followed by carbonization. Companies that currently develop gas diffusion layers based on the dry-laid and hydroentangled nonwoven fabric mat are SGL (Germany) and Freudenberg (Germany).

CHAPTER III

MANUFACTURING, ASSEMBLY AND TESTING OF POLYMER ELECTROLYTE MEMBRANE (PEM) FUEL CELL

This section describes manufacturing and assembly of PEM fuel cell and development of fuel cell tests. Fuel cell performance was tested by using different flow rates.

Assembly of Polymer Electrolyte Membrane Fuel Cell

Each half cell is composed of three distinct main pieces; a polyvinylchloride (PVC) end plate, graphite monolayer flow field plate and nickel current collector. Each piece fits together to form the outer portion of the fuel cell. This assembly allows reactants and products to flow to and from the membrane at the cell center.

The end plates are machined from PVC material. They give mechanical stability to the stack and enable sealing of the different components by compression. Both anode and cathode sides PVC end plates were cut in 152x152 mm which is shown in Figure 3.1.

Figure 3.1 PVC end plate

Nickel current collectors and silicon rubber gaskets were cut to the size according to templates which are shown in Appendix 1. Nickel is chosen due to its high electric conductivity. Silicon is chosen as the material for gaskets due to the fact that it has the right amount of elasticity to compensate for minor surface flaws and unevenness in the graphite plates and to provide seal that will prevent gas leakage. The nickel current collectors and silicon rubber gaskets are shown a in Figure 3.2 (a) and (b).

The next layer in the cell is the monopolar graphite flow field plates. Each graphite flow field conductor plate was cut to the thickness of 0.476 mm (3/16 in). Then, flow fields were cut in the graphite plates. The vertical oxygen side plate's depth is 0.238 mm (3/32 in) and width is 0.32 mm (1/8 in).The serpentine hydrogen side's depth is 0.238 mm (3/32 in) and thickness is 0.32 mm (1/8 in). The air and hydrogen side's graphite flow field plates are shown in Figure 3.3(a) and (b).

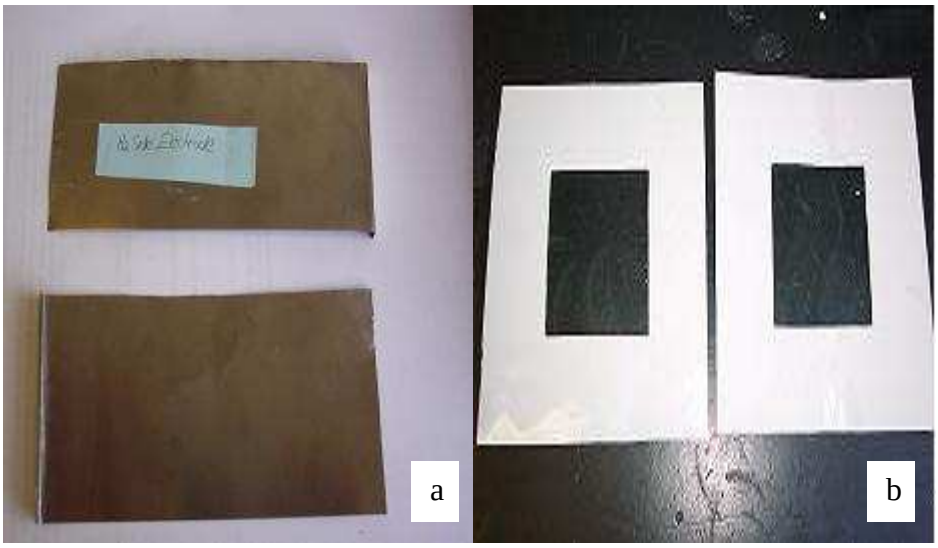

Figure 3.2 (a) Nickel current collectors, (b) Silicon rubber gaskets

0.556 mm (7/32 in) was drilled at each end of the flow field for the fasteners. These holes align with holes in the current collectors and the electrode holder. Fasteners were coated to obtain non-conductivity in the cell.

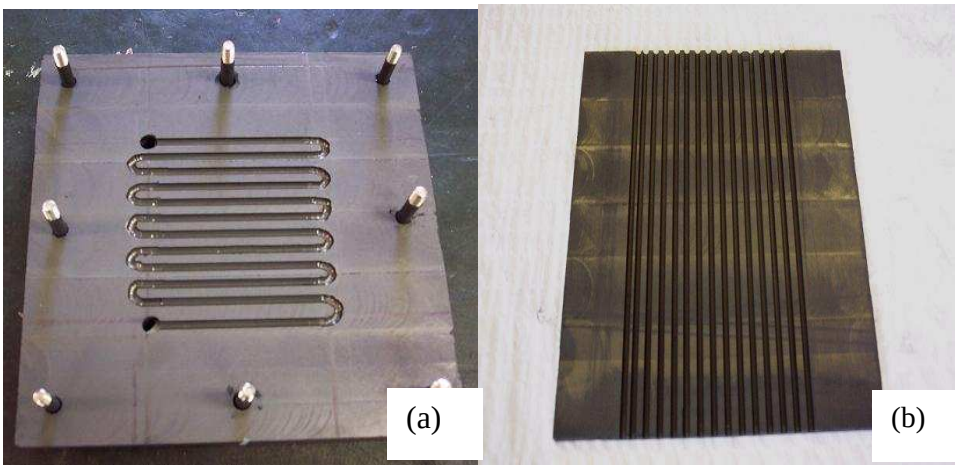

Figure 3.3 (a) Hydrogen flow field plate (b) air flow field plate

Membrane electrode assembly (MEA) is placed between two mylar surrounds, again to prevent any gas reactant leakage. 3L (three layers) SL- 112 MEA that was going to be placed inside the fuel cell body was purchased. The MEA is made up of anode, cathode catalyst layers whose platinum loading is 0.3 mg Pt/cm^2 and Nafion®112

membrane whose thickness is 50 μm. It should be mentioned that there is no gas diffusion layer exist in the MEA and total surface area of the MEA is 50 cm^2.

Before the fuel cell was assembled, the parts had to be cleaned. All the parts are put together as shown in Figure 3.4. The manufactured air/hydrogen polymer electrolyte membrane fuel cell is shown in Figure 3.5 The layers which is shown in numbers are, 1-Assembly bolts 2-Hydrogen side end plate 3-Silicon rubber strip gasket 4-Silicon rubber gasket 5-Hydrogen flow field plate 6-MEA+Mylar gaskets 7-Silicon rubber strip gaskets 8-Air side end plate 9-Air side metal electrode 10-Air flow field plate 11-Hydrogen side metal electrode

Cell compression is achieved by tightening the eight shoulder screws that squeeze against aluminum end plates. Maintaining even pressure over the cell is important to prevent leaks that might be decrease cell performance. In order to achieve even pressure, the screws were cross tightened by hand.

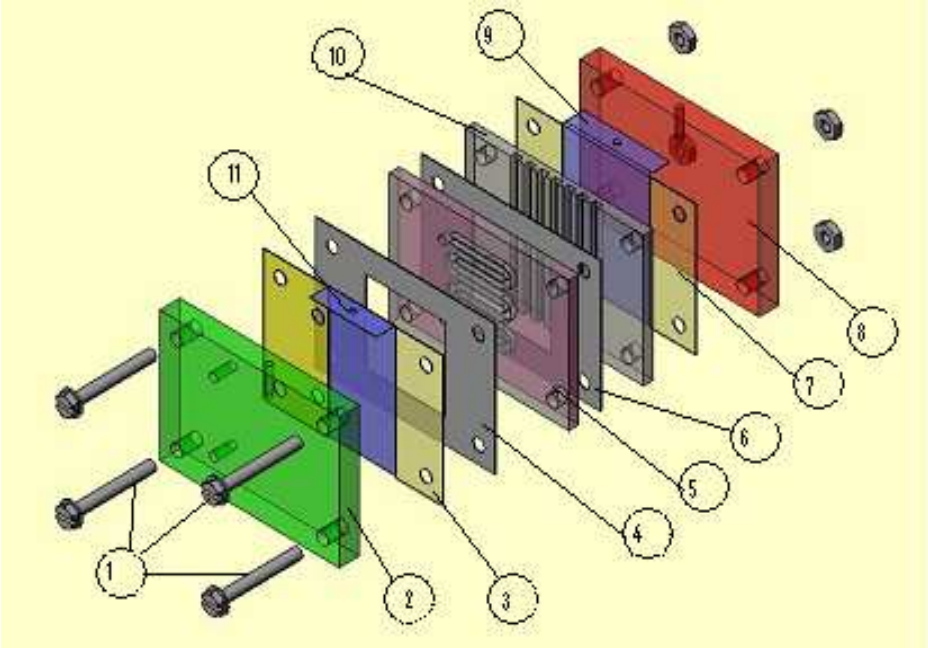

Figure 3.4 Schematic of manufactured PEMFC

Figure 3.5 Manufactured PEMFC

Operation of The Test Stand

Fuel test stand is shown in Figure 3.6. Hydrogen flow rate is independently controlled. There is no station for air flow. Cell temperature and humidification were not controlled for either hydrogen or air side.

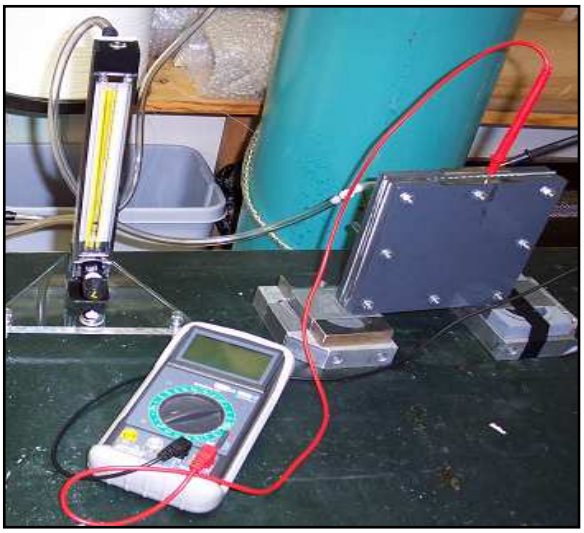

Figure 3.6 Test station

The single air/hydrogen PEMFC was tested at room temperature which is 22˚C. The hydrogen purity was 99.99%. Measuring the cell voltage was done using a model MV 110 digital voltmeter. The current and resistance values were read from the voltmeter under the same conditions.

Results and Discussion

The effects of operating variables ambient air relative humidity and hydrogen flow rate on the performance of air-breathing H_2-air fuel cell are observed.

Water balance in the fuel cell is important although neither cathode nor anode was humidified in the study. Since the flow rate of oxygen is low, it will not dry the membrane as long as the cell is producing power. Water produced by the reaction and carried into the cell by air stream is enough to keep the cell hydrated, due to the thin membrane promoting back diffusion to the anode.

To optimize the cell, voltage responses were collected for a certain time. Figure 3.7 shows the data collected from the cell which was on operation over twenty hours at a

flow rate of 185ml/min.Voltage responses of the cell were recorded in every ten minutes during three hours; then hydrogen feeding was stopped and cell was left idle for three hours (first portion of the graph). This process continued for twenty-one hours and four similar plots were obtained. Figure 3.7 is a proof that the cell has the same trend under the same operating conditions.

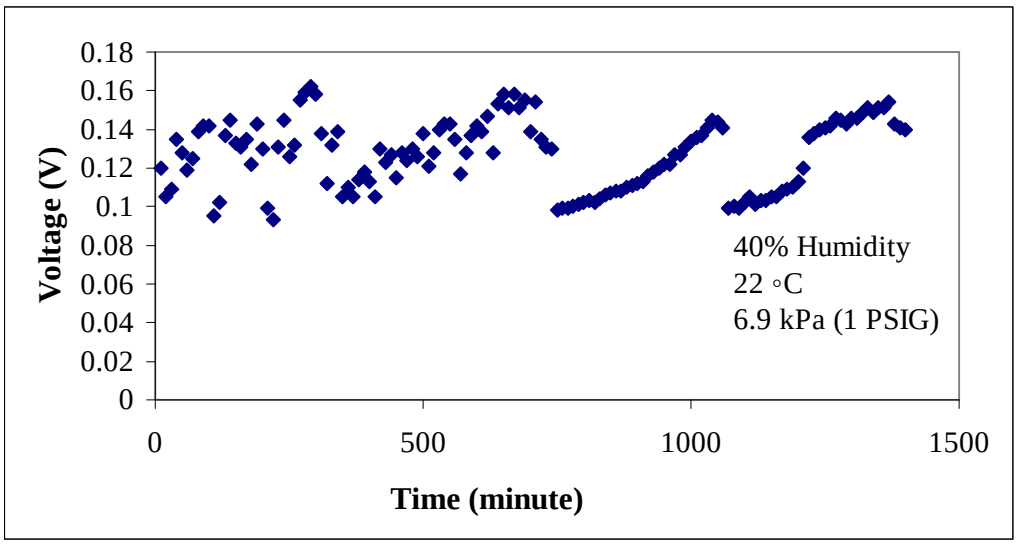

Figure 3.7 The cell performance by time at a flow rate of 185 ml/min

After optimization of parameters such as gauge pressure and hydrogen flow rate, the best performance of the air breathing stack was obtained. Figure 3.8 shows the possible highest voltage output. It is approximately 1.2V at operating conditions of 22°C, 10 ml/min and 70% RH humidity. After 48 hours the cell voltage still remained stable.

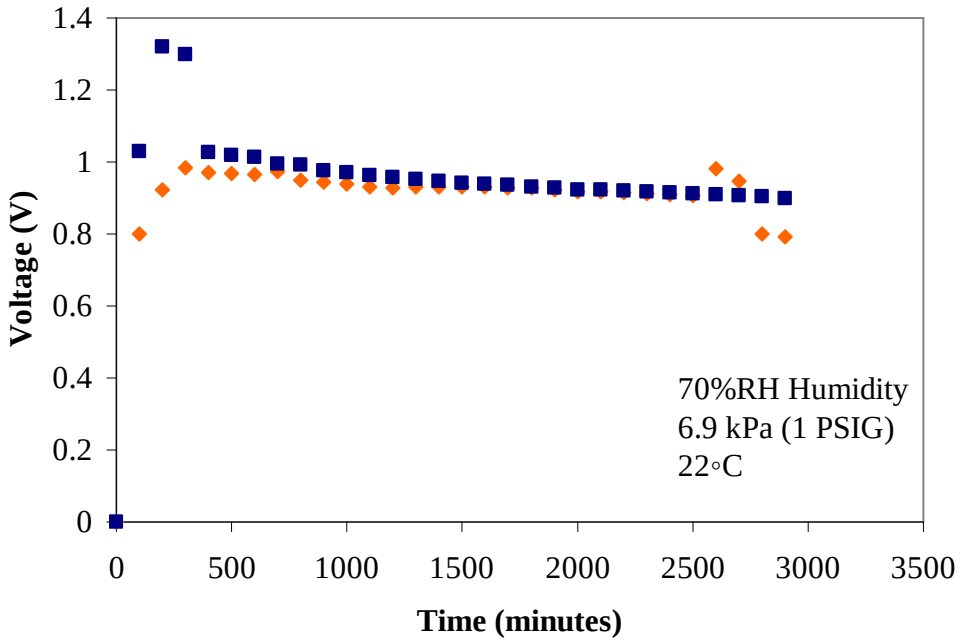

Figure 3.8 Voltage- time behavior of PEMFC at a flow rate of 10ml/min

Different flow rates were used to exam the hydrogen flow rate effect (Figure 3.9). The H_2 flow rates were varied at constant temperature and humidity which is shown in Figure 3.9. It is found that the flow rate has a considerable effect on a single cell voltage; voltage values decrease by an increase in hydrogen flow rate. Maximum cell voltage was obtained at 92 ml/min flow rate as 0.27 V, at 22 ˚C and 40% RH. Figure 3.9 shows that when the flow rate increases from 92 ml/min to 185 ml/min the voltage drops approximately 50%, If too high of a flow rate is applied, the voltage values go almost to zero which is an indication of waste fuel. As explained in Chapter 2, in the part of fuel cross over and internal currents, excess hydrogen passes cross the membrane to the anode side and wastes an oxygen molecule which reacts with electron and causes voltage drop.

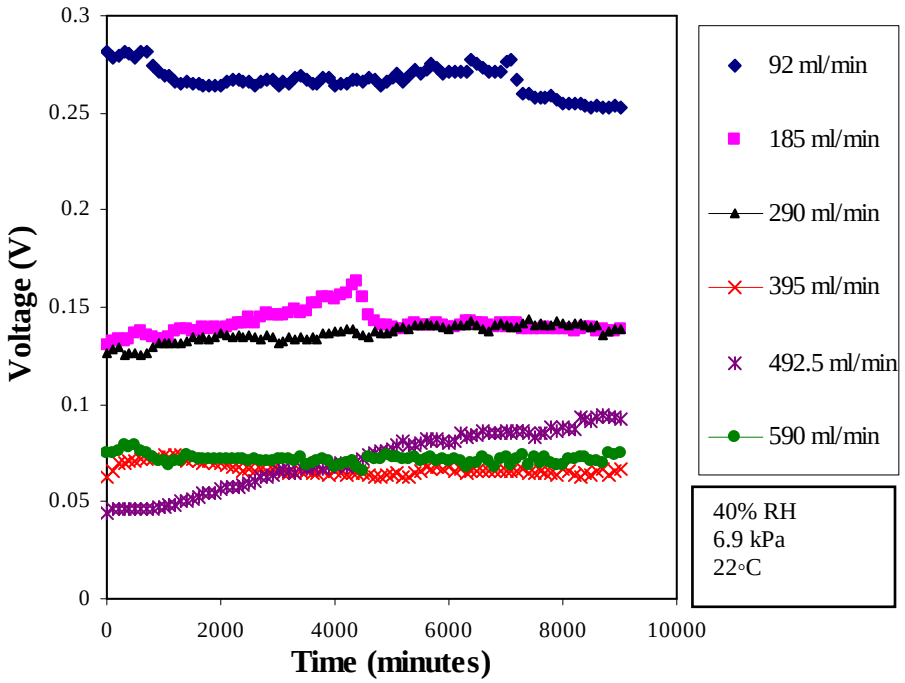

Figure 3.9 Flow rate effect on the cell performance

Different flow rates were applied to the cell at different RH%; room temperature and hydrogen feeding pressure were kept constant. Figures 3.10, 3.11 and 3.12 show voltage, resistance and current values, respectively. Since 1.2 V was observed at 10 ml/min flow rate at 70% RH, low flow rates were applied to the cell. Surprisingly, the same high voltage values could not be obtained at low H_2 flow rates under the same operation conditions. This might be the result of membrane degradation. After all the operations, it was observed that the structure of the MEA in the cell was degraded. The degraded structure is shown in Figure 3.13.

Figure 3.10 shows that the maximum voltage values are observed at 92 ml/min hydrogen flow rate in 75% RH. It should be noted that the resistance values which are shown in Figure 3.11, do not show the total cell resistance. This resistance values were

measured using a digital voltmeter and represent static resistance which depends on the ambient conditions (i.e., temperature, humidity) of the cell.

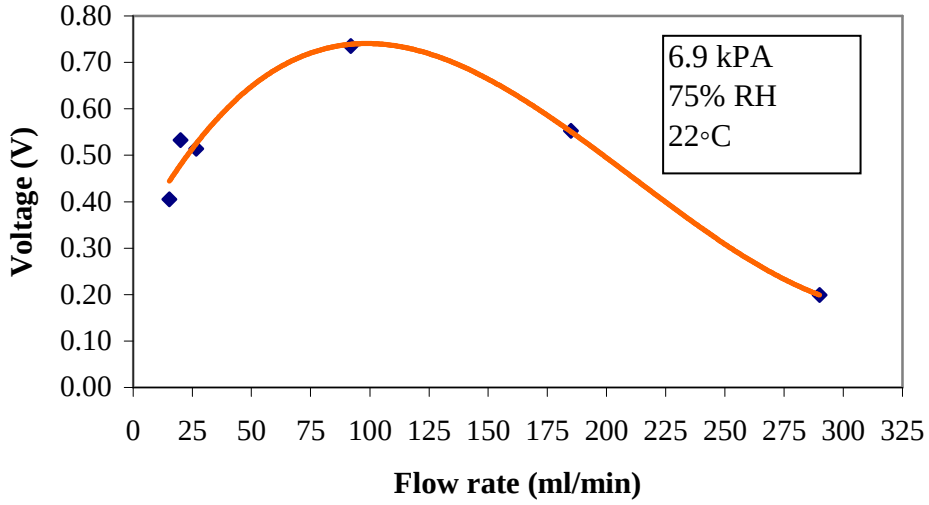

Figure 3.10 Variation of voltage with flow rate

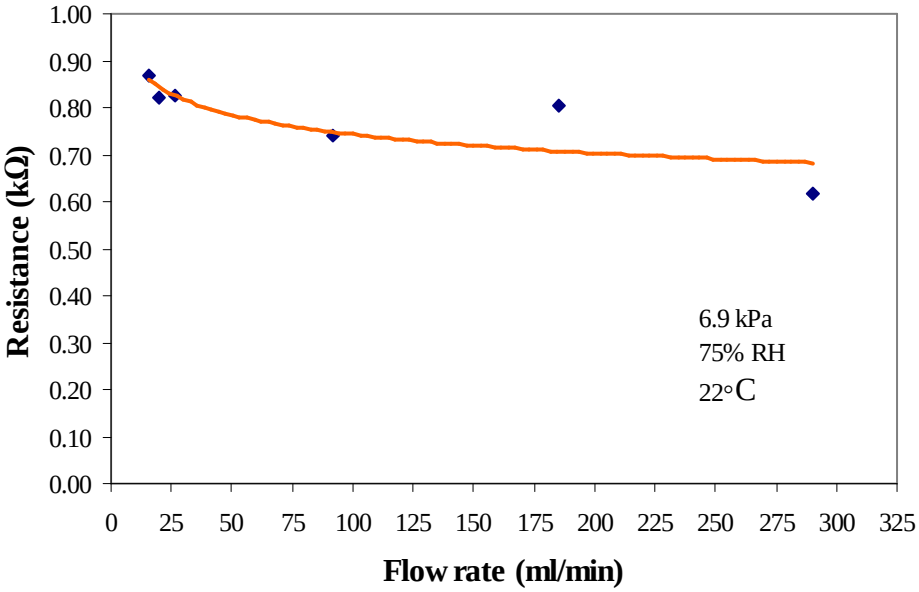

Figure 3.11 Variation of resistance with flow rate

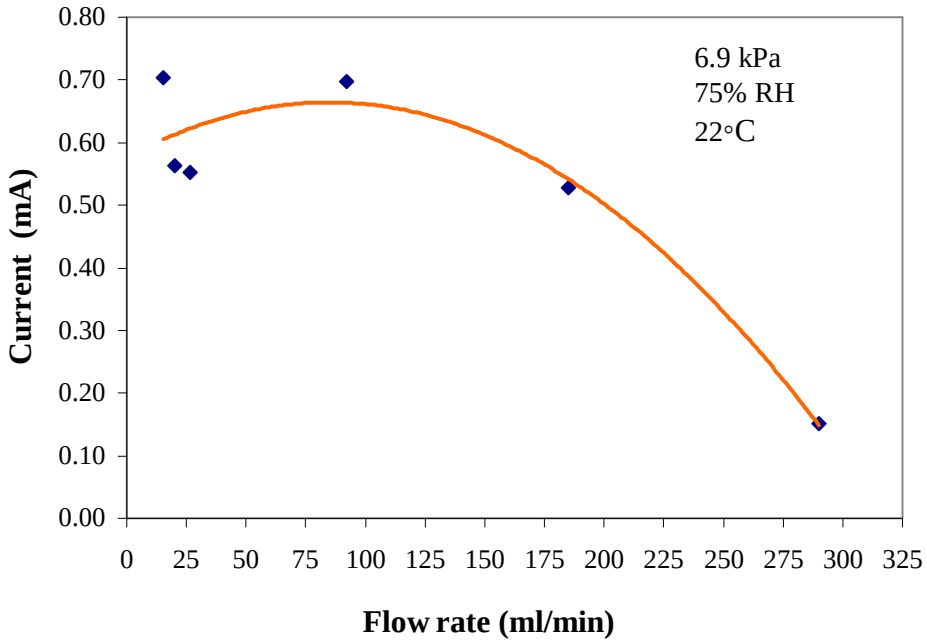

Figure 3.12 Variation of current with flow rate

Additionally, comparison of Figures 3.9 and 3.10 shows ambient humidity effect on the PEM fuel cell performance. The disadvantage of air-breathing fuel cell is that any factor, which may be present in surrounding environment, may affect the cell performance. Figure 3.14 shows the effect of relative humidity (%RH) on the cell voltage at 22°C. The voltage has higher values for different flow rates at 75% relative humidity and the overall voltage values are low at lower humidity (40% RH).

The air-breathing cell was designed to use oxygen from air. The reaction product of water in the cathode was exhausted to the environment which can be seen in Figure 3.15.

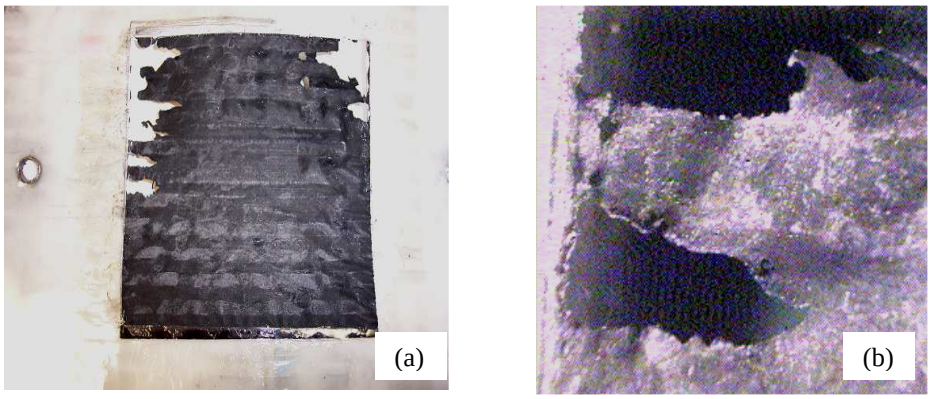

Figure 3.13 (a) Degraded MEA structure and (b) degraded MEA structure 90X magnifications

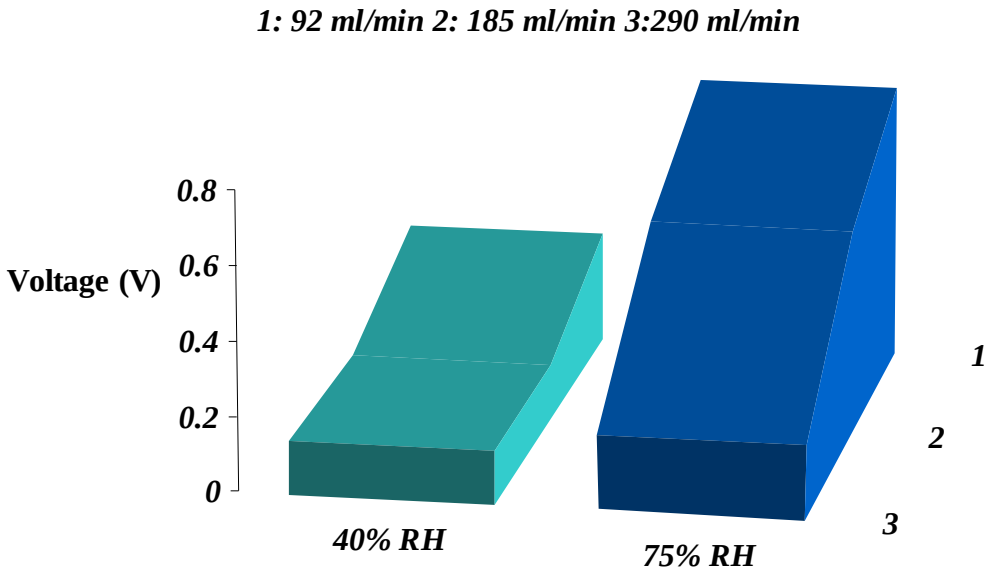

Figure 3.14 Ambient humidity effect on the PEM fuel cell performance

Figure 3.15 Flooding from the manufactured PEM fuel cell

CHAPTER IV

MANUFACTURING AND CHARAZTERIZATION OF GAS DIFFUSION LAYERS FOR PEM FUEL CELLS

Introduction

For high power fuel cells, power levels depend on steady-state heat and mass transfer rates at the electrode-electrolyte interface. New types of materials require advanced flow-through electrode structures which provide controlled wetting to eliminate flooding while at the same time increasing appropriate transport rates which occur at interfacial contact areas between the gaseous reactants and electrocatalysts (i.e., Pt/carbon)

The primary goal in this part of the study was to prepare gas diffusion layers with properties well-suited for particular applications in polymer electrolyte membrane fuel cells.

Firstly, commercially available gas diffusion layers' physical properties were investigated to have better understanding of the structure of gas diffusion layers. Then, a versatile material preparation technique that allows for high degree of flexibility in electrode properties (i.e. specific surface area and electrical conductivity) was utilized. The goal is to overcome major difficulties in fabricating and utilizing high surface area and to obtain high electrical conductivity of carbon gas diffusion layers.

The material presented in this chapter describes procedures for preparing gas diffusion layers from carbon fibers and physical properties of these carbon gas diffusion layers.

Experimental

Initially, the experimental studies focused on determining the structure and physical properties of commercial gas diffusion layers. The common gas diffusion layers were collected; their properties, which were reported by the suppliers, are given in Table 4.1.

Table 4.1 Properties of the commercial GDL structures

Reference GDL Support	***Type***	***Weight (g/m^2)***	***Density (g/cm^3)***	***Thickness (mm)***	***PTFE (%)***
B1A	Plain weave carbon cloth	116		0.35	0
B1C	Satin weave carbon cloth	289		1	20
B1D	Knitted carbon cloth	225		1	20
B2090	Toray carbon paper	225*	0.49 g/cm^3	0.26	20
B2120	Toray carbon paper	290*	0.49 g/cm^3	0.35	20

*Calculated value

Moreover, A-6-P ELAT® V2.1 (hand fabricated, single sided coating) and "E-TEK developmental gas diffusion layer" were used; but their specifications are not given clearly by the suppliers. A-6-P ELAT® V2.1 has Toray carbon paper TGPH-120 whose

thickness is 0.35 mm. Its final thickness varies with catalyst loading and coating. The final sample thickness was measured to be 0.42 mm.

Characterization Method

PEMFC gas diffusion media that includes both gas diffusion layer and gas diffusion electrode is in its early stage of development. Also, there is a little correlation between in-situ and ex-situ performance of the materials [4]. Hence, there are many characterization methods of gas diffusion layers. Through plane electrical conductivity of gas diffusion layer was used in this study.

Through-plane Conductivity

In this method, a sheet of diffusion media is placed between two copper plates, under a defined compression; a d.c. current through the material is applied and plate-to-plate voltage drop is measured. The through-plane conductivity in the z direction is expressed in units of $\Omega.cm^2$. The schematic of the test stand that was developed for this purpose is shown in Figure 4.1

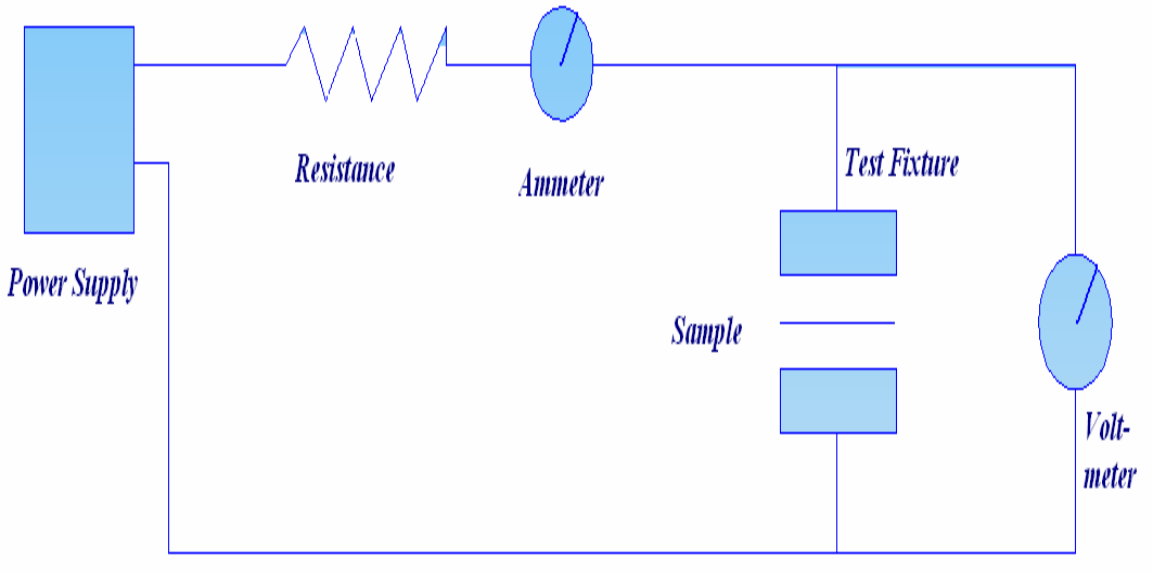

Figure 4.1 Schematic of the through-plane conductivity test stand

E-TEK gas diffusion layers' resistance measurement was done similar to through-plane conductivity test. Compression provided by INSTRON 4505 mechanical bench was used which is shown in Figure 4.2. Samples were directly placed between copper plates without including bipolar plates or any cell part. The compressive pressure was in the range 0-1 MPa.

The measured resistance includes;

1. Bulk material resistance

2. Contact resistance between diffusion paper and plates

The measured resistance in ohms (Ω) can be formulated [19] by

$$R_{Z,meas} = \frac{R_{contact} + R_{Z,bulk}}{A} \qquad [4.1]$$

where A is the area of each gas diffusion media, and $R_{contact}$ represents the plane/diffusion-media contact resistance. To minimize the contact resistance, copper was

chosen as the plate material. The bulk resistance, $R_{Z,bulk}$, contribution can also be expressed as

$$R_{Z,bulk} = \rho_Z \, d \qquad [4.2]$$

where ρ_Z is the through plane resistivity (Ω cm) and d is the material thickness (cm). It should be noted that the contact resistance between diffusion media and the catalyst layer is not considered.

Figure 4.2 Through-plane conductivity measurement on INSTRON 4505 testing device

Results and Discussion

The measured resistance values under different compressions of E-TEK gas diffusion layers are shown in Figure 4.3

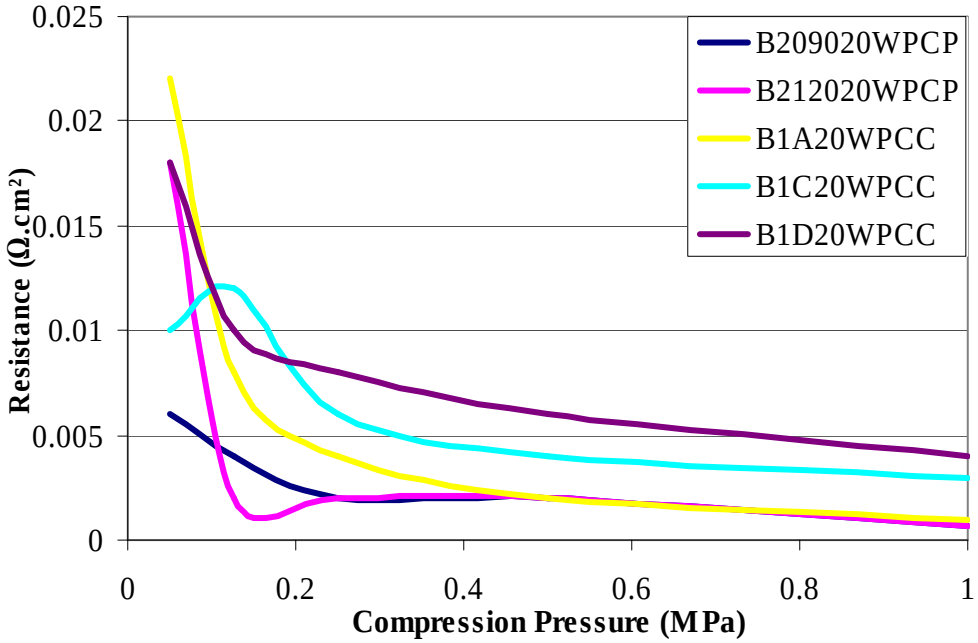

Figure 4.3 Resistance of carbon-fiber gas diffusion layers (E-TEK) as a function of compression pressure

The surface of the gas diffusion layers was observed before and after the compression. The state of the materials after compression is shown in Figure 4.4. Their different behaviors may be related to differences in their microstructures.

Figure 4.3 shows that the measured electrical resistance decreases quickly with the stress applied on the GDL. It can be mainly ascribed to the contact resistance at different interfaces under compression. Concerning the carbon cloth, the highly compressive behavior can easily be explained since it is woven or knitted structure. Even though their initial resistances are high, the fibers are packed together during compression because of porous structure of carbon cloth. Moreover, the interlacing of the cloth increases as the stress increases when two perpendicular yarns are pulled together. Finally, cracks are observed on the carbon cloth after compression. It appears that the

stress applied on the GDLs, to enhance their contact area and electrical conductivity with the bipolar plates and the active layers, could affect the durability of gas diffusion layers.

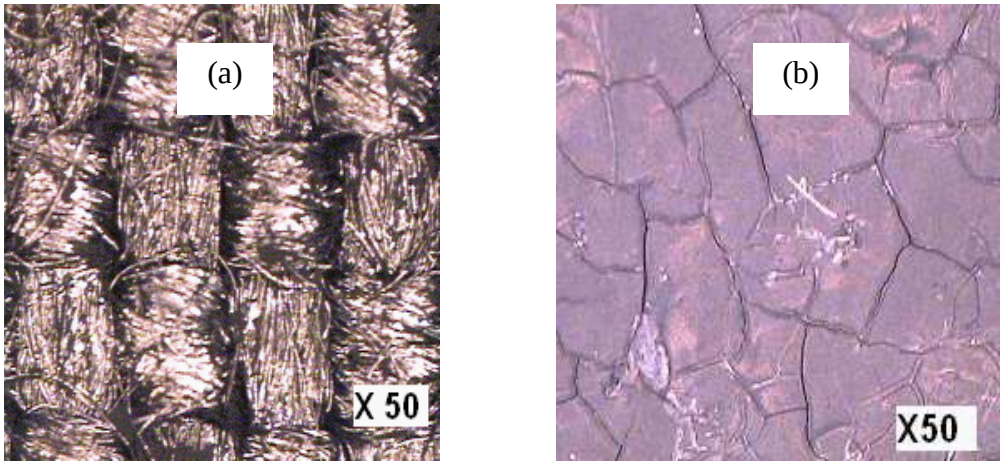

Figure 4.4 Micrographs of carbon cloth (a) and carbon paper (b) gas diffusion layers after compression at 1 MPa

Consequently, carbon paper has the advantage of low resistance under low compression pressure. Thus, manufacturing and evaluation of carbon paper is the next step of the study.

Wet-Laying Process

Materials

The materials used during gas diffusion layer preparation were carbon fibers (Toho Co., LTD.), Kuralon polyviniyl alcohol (PVA) (Kuraray Co., LTD.) and wood cellulose fibers. Individual carbon fibers are 7 μm in diameter and 6 mm in length. PVA fibers are 17μm in diameter and 6 mm in length and cellulose fibers are 20-30 μm in diameter and varied in length from 100 to 1000 μm.

For coatings and treatments, DuPont Teflon® PTFE TE-3859, conductive epoxy binder (Creative materials, Inc.) and Polyviniyl alcohol (PVA) with a molecular weight of 95000 were used.

Fiber Preparation

Before the fiber materials were combined into a paper form, cellulose fibers were soaked into water for twenty-four hours for swelling. Zhang et al. [28] studied the impregnation of carbon fibers with NaOH for better water uptake in the gas diffusion layer. They stated that their manufactured carbon paper is the perfect raw material for the electrode diffusion layer of fuel cells. Thus, in the samples, NaOH impregnated carbon fibers were used. Carbon fibers were left in 10% NaOH solution for twenty-four hours. The list of fiber content and weight of samples can be seen in Table 4.2

Formation of Paper Form

During manufacturing, different combinations of fibers were used. The fiber contents and operation conditions are listed in Tables 4.2, 4.3 and 4.4. The following are some examples of the manufactured gas diffusion layers.

Table 4.2 Bulk composition and drying temperature of manufactured fiber blend composite paper gas diffusion layer

Sample	***Fiber Content***	***Amount of Fibers (g)***	***NaOH (3 Molar)***	***Drying Temperature (°C)***
1	C	1	Yes	100
2	C	1	No	100
3	C	2	No	100
4	C+Cel	1+0.5	No	100
5	C+PVA	1+0.25	No	200
6	C+PVA	1+0.5	No	200
7	C+PVA	1+1	No	220
8	C+PVA	1+1	No	240
9	C+PVA+Cel	1+0.25+0.25	No	200
10	C+PVA+Cel	1+0.25+0.10	No	200
11	C+PVA+Cel	1+0.25+0.05	No	200

C: Carbon fiber Cel: Cellulose fiber PVA: Polyvinyl alcohol fiber

Table 4.3 Bulk composition of manufactured coated composite carbon paper gas diffusion layers

PTFE: Polytetrafloraethylene PVA: Polyvinylalcohol

Sample	***Fiber content***	***Amount of fibers(g)***	***Coating***	***Molding***	***Drying Temp. (°C)***
12	C	1	10% PVA	-	200
13	C	1	10% PVA	-	220
14	C	1	10% PTFE	-	235
15	C	1	10%Conductive Pol. 10% PTFE	+	70
16	C	1	10% PVA	+	150

Table 4.4 Bulk composition of C/PVA/Cellulose fiber blend carbon papers

Sample	***Fiber Content***	***Blend Ratio (%)***	***Drying Temperature (◦C)***
17	C+PVA+Cel	50:00:50	140
18	C+PVA+Cel	50:10:40	140
19	C+PVA+Cel	50:20:30	140
20	C+PVA+Cel	50:30:20	140
21	C+PVA+Cel	50:40:10	140
22	C+PVA+Cel	50:50:00	140

It should be noted that the results are the average of three values.

Example 1

1.0 g chopped carbon fibers, 0.5 g PVA fibers and 0.5 g cellulose fibers were dispersed in 1 liter of water using a standard catering blender. The resulting dispersion was used to produce a nonwoven sheet of 200 cm^2 using a sheet mold which is shown in Figure 4.5.

Figure 4.5 Sheet mold

The wet paper composite is pressed at 400 kN/m^2 and the sheet is dried at 200 $^{\circ}$C in air.

Example 2

1.0 g carbon fibers and 1 liter of 10% PVA solution were agitated in the blender. The dispersed fiber mixture was further diluted and formed in a sheet mold (200 cm^2). The wet paper composite is left to air dry for twenty-four hours. Then, in the compression molding machine, heat was applied gradually from room temperature (22 $^{\circ}$C) to 150 $^{\circ}$C under 2.26 MPa (328 PSI). After reaching 150 $^{\circ}$C, heating was stopped and the paper was left to cool down to the room temperature under the same pressure.

Example 3

5% conductive resin and 10% PTFE were diluted in 1 liter water, agitated in the blender with 1 g carbon fibers and formed in the sheet mold (200 cm^2). The paper composite is left to air dry for twenty-four hours. Similar to Example 2, composite paper was gradually dried from 22 $^{\circ}$C to 70 $^{\circ}$C. After reaching 70 $^{\circ}$C, the paper was left to cool down to its initial temperature under the same pressure. The schematic of compression molding is shown in Figure 4.6.

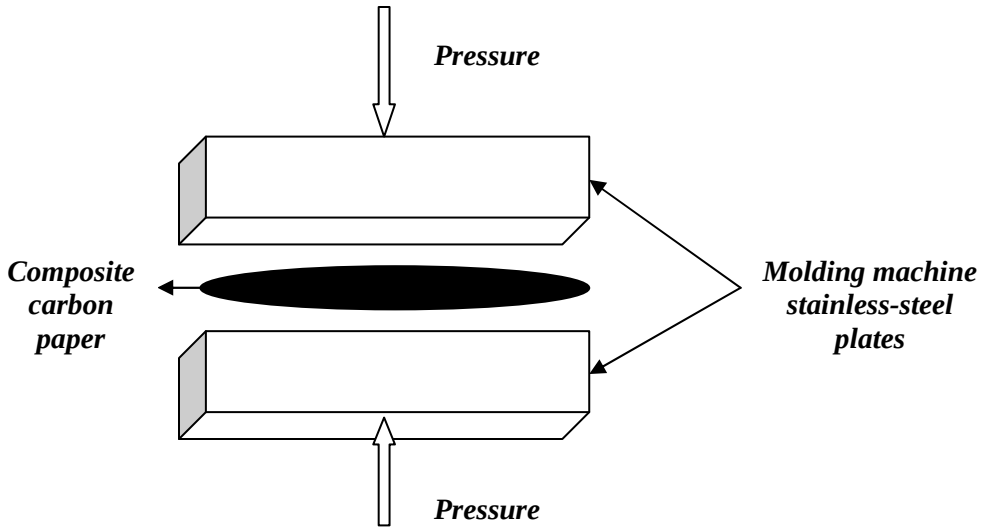

Figure 4.6 Schematic of the compressing molding machine

Characterization

Resistance tests of manufactured carbon paper samples were done according to the through-plane resistance test on Instron 4505. The strength and thickness of manufactured carbon papers were measured according to ASTM D 5035 and D 1777. In ASTM D 5035, which is called the strip test, the size of the samples used were as follows: width 25.4 mm, length 50.8 mm, instead of 25.4 mm and 76.2 mm, respectively.

The morphology of manufactured gas diffusion layers was observed with scanning electron microscope (SEM). The sample was mounted on the sample holder and sputter-coated with gold before placement in the SEM to observe the arrangement of the carbon fibers in the paper.

Results and Discussion

In Figure 4.3, it is observed that after 0.30 MPa, the resistance of the manufactured carbon papers is almost stable so that for resistance measurements, 0.25 MPa was chosen as the compression pressure. The properties of the manufactured carbon

papers are shown in Table 4.5. To obtain more accurate results, each sample was manufactured three times and the average value is reported.

Table 4.5 Properties of the manufactured gas diffusion layers

Sample	***Thickness (mm)***	***Resistance (Ωcm²)***	***Strength (kgf)***
1	0.78	0.56	0.02
2	0.65	0.06	0.02
3	0.72	0.28	0.02
4	0.73	1.48	0.10
5	0.99	0.52	0.08
6	1.24	0.60	0.08
7	1.87	0.64	0.08
8	1.85	0.6	0.08
9	1.23	0.48	0.09
10	1.10	0.48	0.06
11	1.04	0.48	0.04
12	0.6	1.28	1.10
13	0.79	0.96	2.00
14	0.80	0.20	0.04
15	0.47	0.96	2.05
16	0.39	0.68	1.50
17	1.10	0.72	0.77
18	0.99	0.72	0.36
19	1.71	0.64	0.23
20	0.85	0.60	0.14
21	1.35	0.24	0.07
22	1.80	0.68	0.03

The characterization of different gas diffusion layers with through plane resistance method was done in the study. The electrical conductivity and morphology of five different commercial gas diffusion layers were compared with 22 manufactured carbon papers. Uncompressed thickness and resistance values of both commercial and

manufactured macroporous gas diffusion layers were compared in Figure 4.7. It is found that there is no correlation between GDL's initial thickness and its resistance (Ω cm^2).

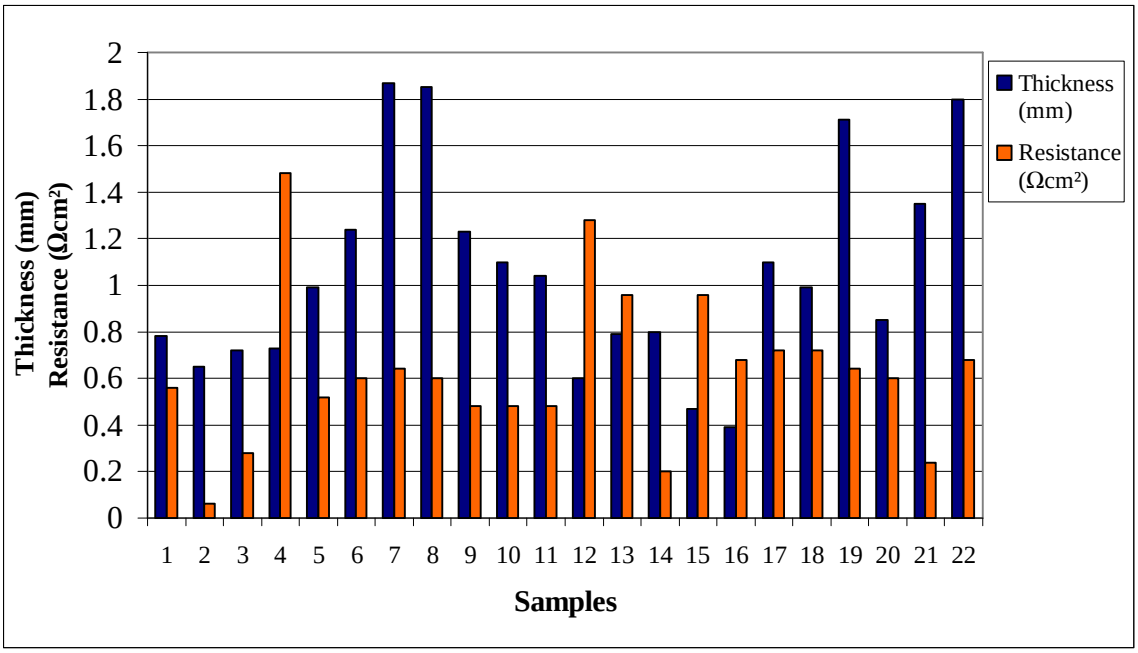

Figure 4.7 Thickness and resistance values of the manufactured carbon papers

Since carbon fibers have low friction, PVA and cellulose fibers were blended to enhance strength properties of carbon papers. Strength and resistance values are shown in Figure 4.8. To have optimum strength and resistance values, different fiber blends and coatings were studied.

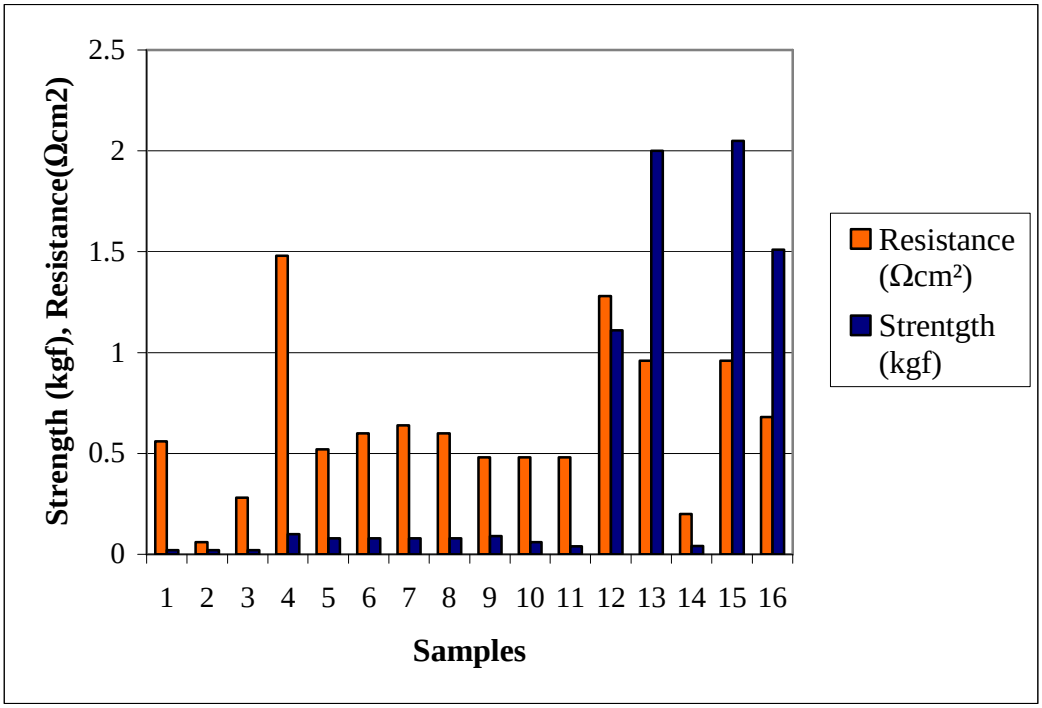

Figure 4.8 Resistance and strength values of the manufactured carbon papers

As mentioned earlier, Zhang et al. [28] studied NaOH impregnation of carbon fibers, to optimize water uptake in MEA. If sample 1 and sample 2 are compared in Figure 4.8, it is seen that NaOH has a positive effect on resistance. Resistance increases 50% in NaOH impregnated carbon fiber paper. Surface characterization of the NaOH impregnated carbon fiber paper is shown in Figure 4.9 (a). NaOH particles remained on the carbon fibers. NaOH can be hydrolyzed in the open air and washed out by water. It is reasonable to state that the durability of the NaOH particles in the carbon paper is unpredictable since there is no interaction between carbon fibers and NaOH particles.

If sample 2 and sample 4 are compared, it can be observed that carbon/cellulose blended carbon paper has better strength. Its strength is 5 times higher than that of the unblended carbon fiber paper (sample 2); on the other hand, its resistance is approximately 20 times higher than the unblended carbon paper.

PVA has a water soluble molecule; the most important change is the increase of crystallinity of PVA through the removal of residual water and the formation of new hydrogen bonds between PVA molecules. Thus, heat treatment of the PVA molecules turns the water-soluble-polymer to water-insoluble polymer. Depending on the cyrstallinity, melting point ranges from 180 °C to 240 °C [29]. In this study, carbon/PVA fibers blend carbon papers (samples 6, 7, 8) were heat treated from 200°C to 240 °C as shown in Table 4.1. Figure 4.9 (b) shows the surface morphology of carbon/PVA blend carbon papers which was dried at 200 °C in the air. It is observed that there is no physical interaction between carbon and PVA fibers. Another proof is the samples' (samples 6, 7, 8) strength results which are shown in Figure 4.8. Strength improvement of the carbon/PVA blended fibers paper is not significant. Untreated PVA fibers are shown in Figure 4.10 to compare the surface of heat treated and untreated PVA fibers.

To improve strength values, experimental polymer coating (Creative Materials, product number 111-05) was applied to the carbon papers. For coating, PVA powder were dissolved in water. PVA coated carbon paper's micrograph is shown in Appendix B. Samples 12 and 13 are compared to observe the effect of PVA coating on carbon paper. In contradiction to carbon/PVA fiber blend carbon paper, drying temperature has a distinct effect on strength and resistance; 10% increase in temperature (from 200°C to 220°C) enhances the strength by 100% and decreases the resistance by 33%.

PTFE was also applied as coating; but, as it is seen in Figure 4.11, there is no PTFE coating remains on the carbon paper surface (Sample 14). Addition of the conductive polymer from Creative Materials has a positive effect. While it decreases the

resistance, the strength value remains the same as that of 10% PVA coated sample (Sample 15). The photo-migrograph of Sample 15 is shown in Appendix B.

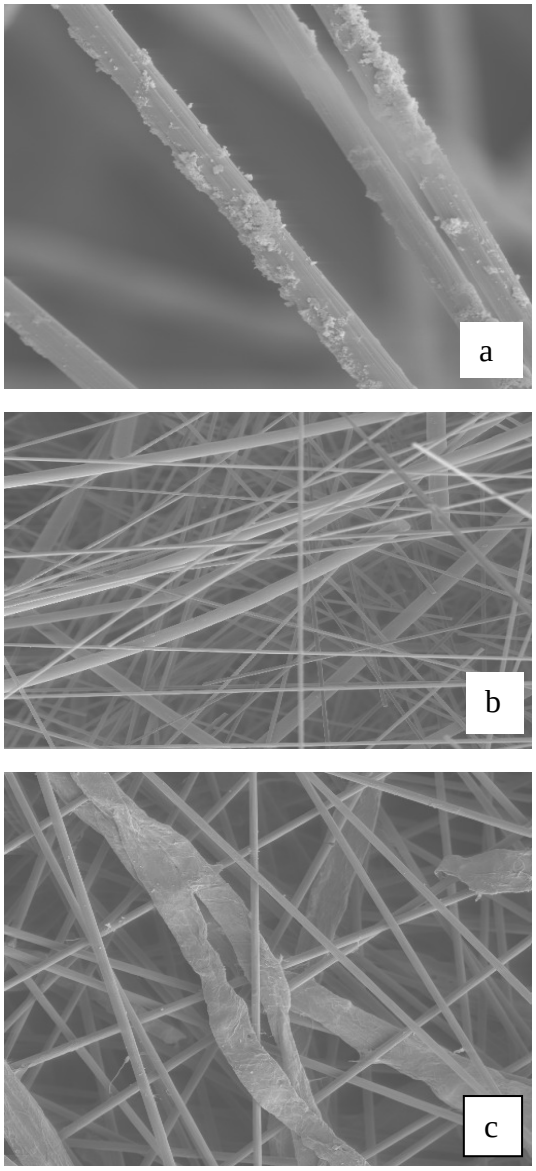

Figure 4.9 SEM pictures of (a) carbon fiber with NaOH impregnation, 1000X (b) carbon and PVA fibers blend, 100X (c) carbon and cellulose fibers blend, 200X

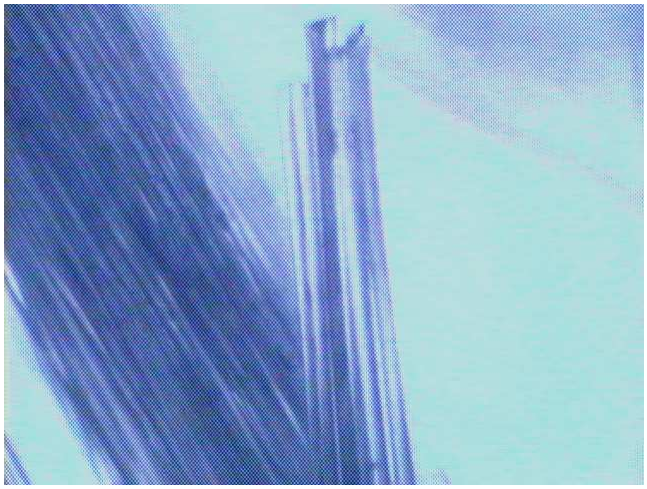

Figure 4.10 Photo-micrograph of untreated PVA fibers (90X)

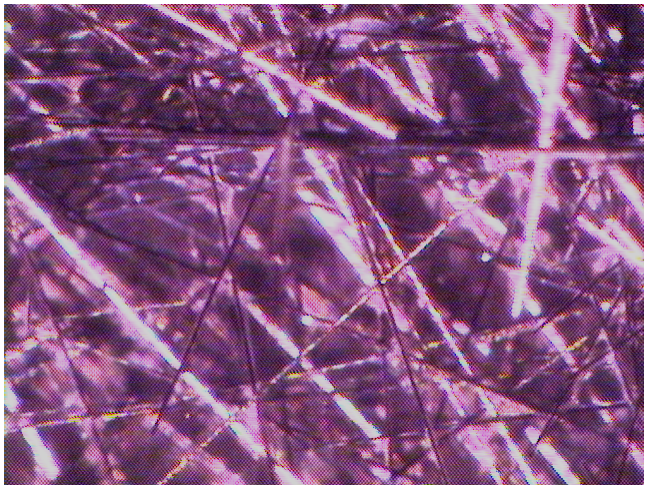

Figure 4.11 Photo-micrograph of Sample 14 (90X)

Figure 4.9 (c) shows the interaction between the carbon and cellulose fibers in the blended carbon paper (Sample 4). Similar to the carbon/PVA blend, it is observed that there is no interaction between carbon and cellulose fibers and the strength of this carbon paper comes from interaction between the cellulose fibers.

Figure 4.12 shows the PVA and cellulose fibers ratio effect on the resistance and strength values of carbon papers. It might be expected that PVA and cellulose fibers' contributions to the resistance are different, since resistance decreases with a reduction in

cellulose fiber ratio and an increase in PVA fiber ratio in the carbon paper. But if, Sample 17 (0% PVA) and Sample 22 (0% cellulose) are compared, it is seen that they have approximately the same resistance values. If Samples 17, 18, 19, 20, 21 and 22 are compared, it is seen that when the cellulose ratio decreases (PVA fiber amount increases) the resistance and strength of the carbon paper decrease.

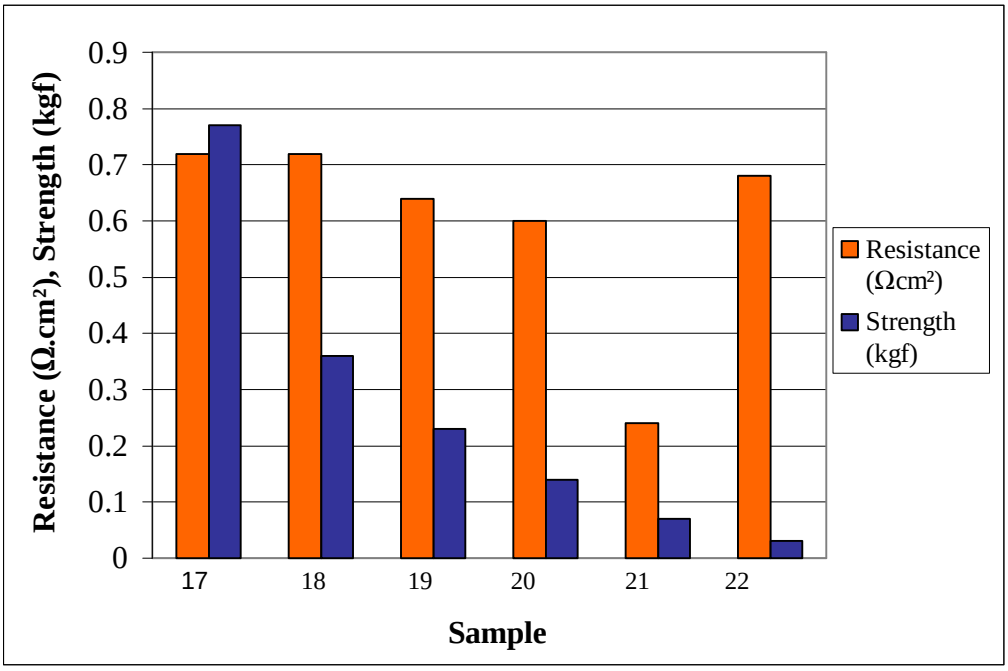

Figure 4.12 Effect of PVA and cellulose fibers blend ratio on resistance and strength

Figure 4.13 shows that the resistance of the manufactured carbon papers and commercial gas diffusion layers are comparable. However, the manufactured carbon paper which approaches to the resistance of the commercial carbon paper for gas diffusion layer, has lower strength values. If Sample 2 and Sample B1A20WP are compared, it is seen that they have similar resistance and strength values.

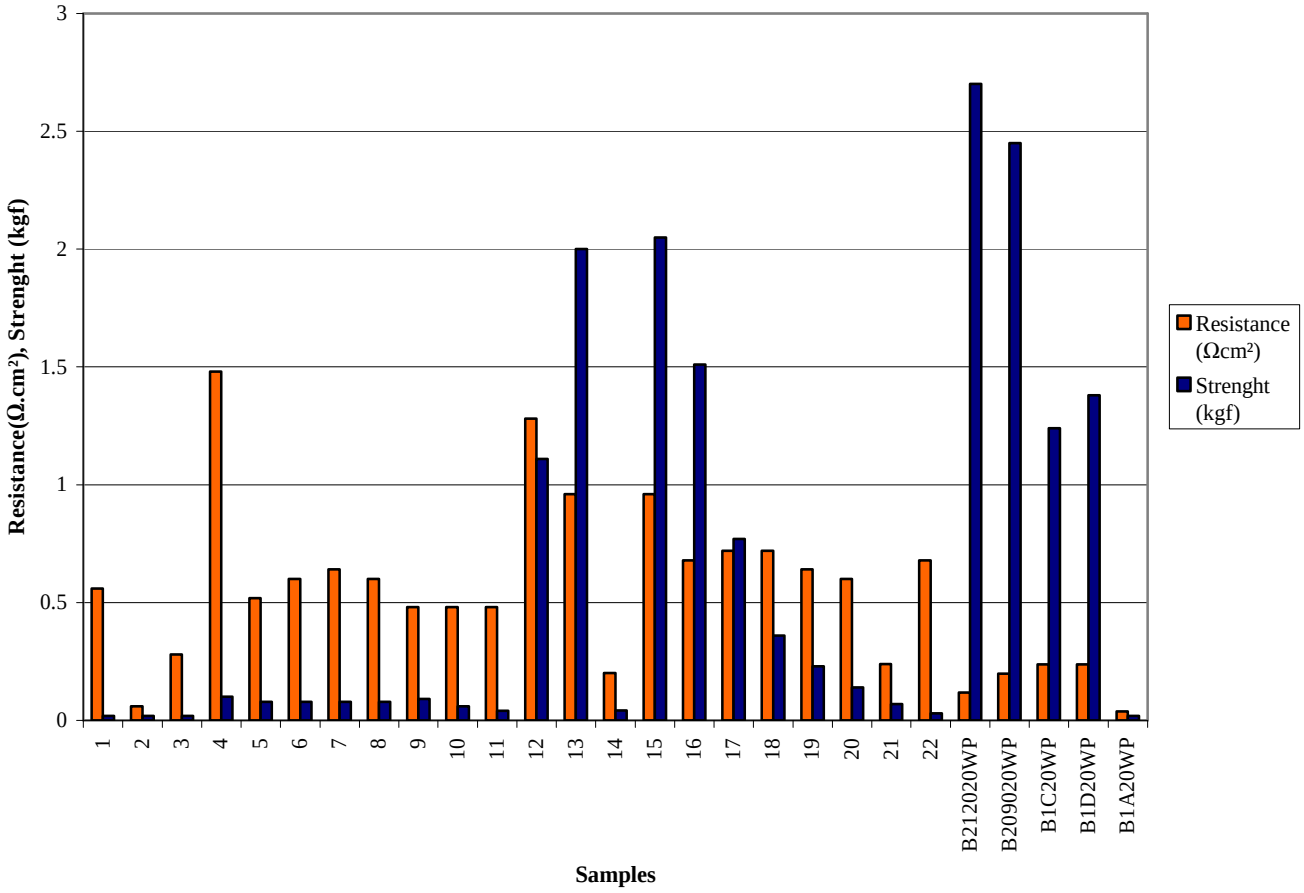

Figure 4.13 Through-plane resistance of commercial and manufactured gas diffusion layers

REFERENCES

1. Thomas, S., and Zalbowitz, M., “Fuel cells–green power”, Los Alamos National Laboratory
2. 2000 Annual Progress Report, U.S. Department of Energy, Energy Efficiency and Renewable Energy Office of Transportation Technologies, October 2000
3. “Fuel cell transit buses”, Hydrogen Fuel Cells and Intrastructure Technologies Program, U.S. Department of Energy, Efficiency and Renewable Energy program,
4. Fuel Cell Handbook, 6th edition by EG&G Technical Services, Inc, November 2002
5. Gode, P., “Investigation of proton conducting polymers and gas diffusion electrodes in the polymer electrolyte fuel cell”, Department of Chemical Engineering and Technology, Applied Electrochemistry, Kungliga Tekniska Högskolan, Stockholm, Doctoral Thesis ,2004
6. Larminie, J., and Dicks, A., Fuel Cell Systems Explained (2nd Edition). John Wiley & Sons, 2003.
7. Ahn, S., “Fiber-based metal-carbon composite electrode structures for fuel cell applications”, PhD, Dissertation, Auburn University, 1992.
8. Kim, J., Lee, S. M., and Srinivasan, S., “Modeling of Proton Exchange Membrane Fuel Cell Performance with an Empirical Equation”, J. Electrochem. Soc., Volume 142, Issue 8, pp. 2670-2674 (August 1995).

9. Chahine, R., Laurencelle, F., Hamelin, J., “Characterization of a Ballard MK5-E Proton Exchange Membrane Fuel Cell Stack”, Fuel Cells, 1 (1) 2001, 66-71.

10. Hoogers G., Fuel Cell Technology Handbook, Florida: CRC press, 2003.

11. Gottesfeld, S. and Zawodzinski, T., “Polymer electrolyte fuel cells”, Adv. Electrochem. Sci. Eng., 5, 1997, 195-301.

12. Mauritz , K., “Nafion”, Chemical Pysics Letters, 379, 2003, 99-104.

13. Banerjee, S., Curtin, D. E., “Nafion® perfluorinated membranes in fuel cells”, Journal of fluorine chemistry, 2004, vol. 125, n 8, pp. 1211-1216.

14. Nemat-Nasser, S., and Thomas, C., W., “Chapter 6: Ionomeric Polymer-Metal Composites”, University of California, San Diego, 2001

15. Rajendran, R., “Polymer electrolyte membrane technology for fuel cells”, Mrs. Bulletin, V. 30, August 2005, page 587-590.

16. Alberti, G., and Casciola, M., “Composite membranes for medium-temperature PEM fuel cells”, Annual Review of Materials Research, Vol. 33, pg. 129-154.

17. Glipa, X., Hogarth, M., Department of Trade and Industry (UK) Homepage, 2001. Available from http://www.dti.gov.uk/renewable/pdf/f0200189.pdf, accessed 04/08/2007

18. Mehta, V., and Cooper J.,S., “Review and analysis of PEM fuel cell design and manufacturing”, Journal of Power Sources, V. 114, 2003, pg. 32-53.

19. Mathias, M., Roth, J., Fleming, J., and Lehnert, W., “Chapter 46: Diffusion media materials and characterization”, Handbook of Fuel Cells, Fundamentals, Technology and Applications, Edited by Wolf Vielstich, Hubert A. Gasteiger,

Arnold Lamm. Volume 3: Fuel Cell Technology and Applications, 2003, John Wiley & Sons, Ltd

20. ” Escribano, S., Morin, A., Mosdale, R., **“**Characterization of PEMFCs gas diffusion layers properties”, *Journal of Power Sources*, V. 156, n 1, May 19, 2006, p 8-13.
21. Roshandel, R., Farhanieh, B., Saievar-Iranizad, E., “The effects of porosity distribution variation on PEM fuel cell performance**”,** Renewable Energy, Volume 30, Issue 10, pages 1557-1572
22. Lee, W., Ho, C., Van Zee, J.W., Murthy, M., “The effects of compression and gas diffusion layers on the performance of a PEM fuel cell”, Journal of Power Sources, V. 84, 1999, pg. 45–51
23. Sun, W., Peppley, B., and Karan, K., Journal of power Source, 2005, v. 144, pg. 42-53
24. Ihonen, J., Mikkola, M., Lindbergh, G., “Flooding of gas diffusion backing in PEFCs”, Journal of The Electrochemical Society, v. 151, 2004, pg. A1152
25. Walsh J. P.,”Carbon Fibers”, ASM Handbook, V. 21, pg 35-40, 2001
26. Yu, J., Yoshikawa Y., Matsuura, T., Islam, M.N., Hori M., “Preparing gas-diffusion layers of PEMFCs with a Dry Deposition Technique”, Electrochemical and Solid-State Letters, V. 8, n. 3, A152-A155, 2005
27. Chu, D., Jiang, R., “Performance of polymer electrolyte membrane fuel cell (PEMFC) stacks: Part I. Evaluation and simulation of an air-breathing PEMFC stack”, Journal of Power Sources, Volume 83, Number 1, October 1999, pp. 128-133.

28. Zhang, W., Wang, S., Liu, H., Pan, H., “Preparation and performance test of special carbon paper materials for proton exchange membrane of fuel cell”, Taiyangneng Xuebao/Acta Energiae Solaris Sinica, v 27, n 2, February, 2006, pg. 199-202
29. Williams, M. C., “Status of fuel cell development in the United States”, Materials Technology, v 10, n 5-6, May-Jun, 1995, pg 104-112.
30. www. Princeton.edu/~ dcahan/fuelcells , “ What is fuel cell?”, accessed 09/02/2005
31. Arico, A., (Dipartimento di Chimica, Universita 'La Sapienza'); Bruce, P., Scrosati, B., Tarascon, J.M., Van, S., “Nanostructured materials for advanced energy conversion and storage devices”, Nature Materials, v. 4, n. 5, May, 2005, pg 366-377.
32. Pharoah, J. G., (Queen's-RMC Fuel Cell Research Centre); Karan, K.; Sun, W. “On effective transport coefficients in PEM fuel cell electrodes: Anisotropy of the porous transport layers”, Journal of Power Sources, v 161, n 1, Oct 20, 2006, pg 214-224
33. Zhang, X., (Inst. of Carbon Fiber and Composites, Beijing Univ. of Chemical Technology) and Shen, Z., “Carbon fiber paper for fuel cell electrode”, Fuel, v 81, n 17, December, 2002, pg 2199-2201
34. Koseki, K.; Nishihara, H.; Shundo, H.; Nakanishi, T. “Molten carbonate fuel cells with electrolyte plates prepared with paper-making method” Energy Conversion Engineering Conference, 1989. IECEC-89. Proceedings of the 24th Intersociety Volume , Issue , 6-11 vol.3 Aug 1989, Pg.1529 – 1534.

35. Lee, W., (Univ of South Carolina), Ho, C., Van Zee, J.W., Murthy, M., “Effects of compression and gas diffusion layers on the performance of a PEM fuel cell”, Journal of Power Sources, v 84, n 1, Nov, 1999, pg 45-51

36. Gurau, V., (Chemical Engineering Department, Case Western Reserve University); Bluemle, M. J., De Castro, E. S., Tsou, Y., Mann Jr., J. A., Zawodzinski Jr., T. A., “Characterization of transport properties in gas diffusion layers for proton exchange membrane fuel cells. 1. Wettability (internal contact angle to water and surface energy of GDL fibers)”, Journal of Power Sources, v 160, n 2 SPEC. ISS., Oct 6, 2006, p 1156-1162.

37. Williams, M., Begg, E., Bonville, L., Kunz, H. R., Fenton, J. M., “Characterization of gas diffusion layers for PEMFC”, Journal of the Electrochemical Society, v 151, n 8, 2004, p A1173-A1180

38. US Patent 6,949,308

39. US Patent 6,991,870

40. Bessette, R. R., Medeiros, M. G., Patrissi, C. J., Deschenes, C. M., and LaFratta, C.N., “Development and characterization of a novel carbon fiber based cathode for semi-fuel cell applications” Journal of Power Sources, v 96, n 1, Jun 1, 2001, p 240-244.

APPENDIX A: Schematics of The Manufactured PEM Fuel Cell Layers

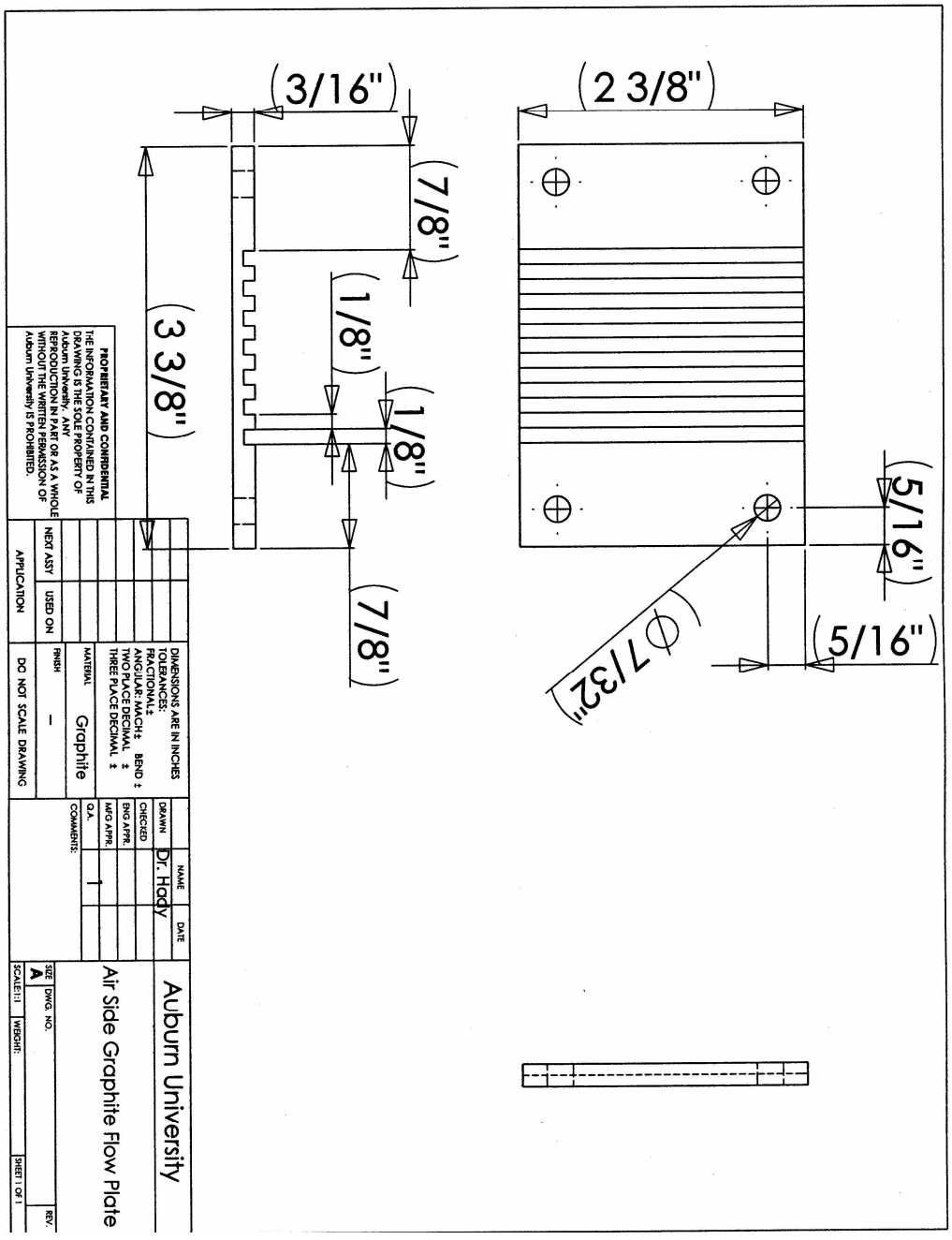

Figure A-1 Air Side Graphite Flow Plate

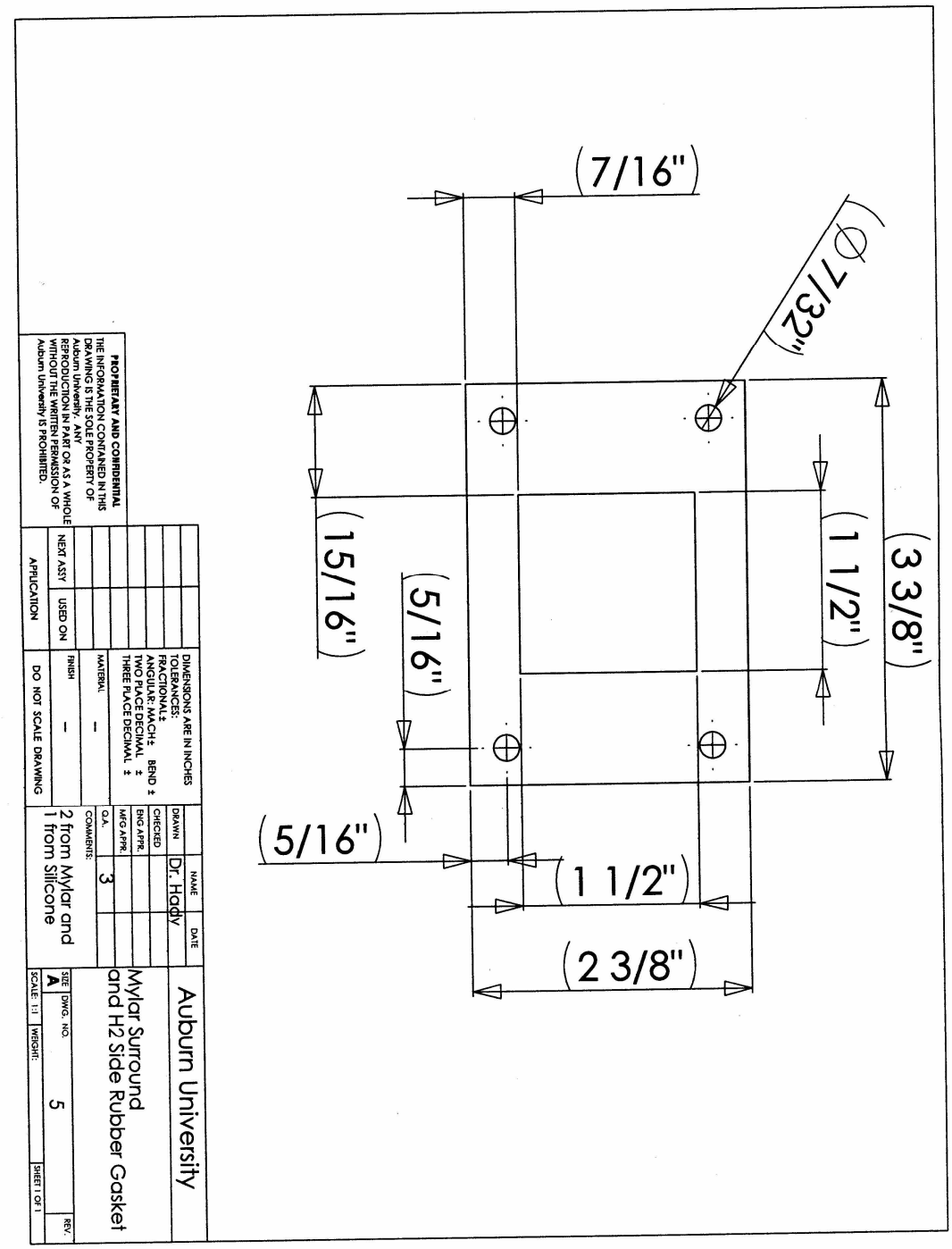

Figure A-2 Mylar surround and H_2 side rubber gasket

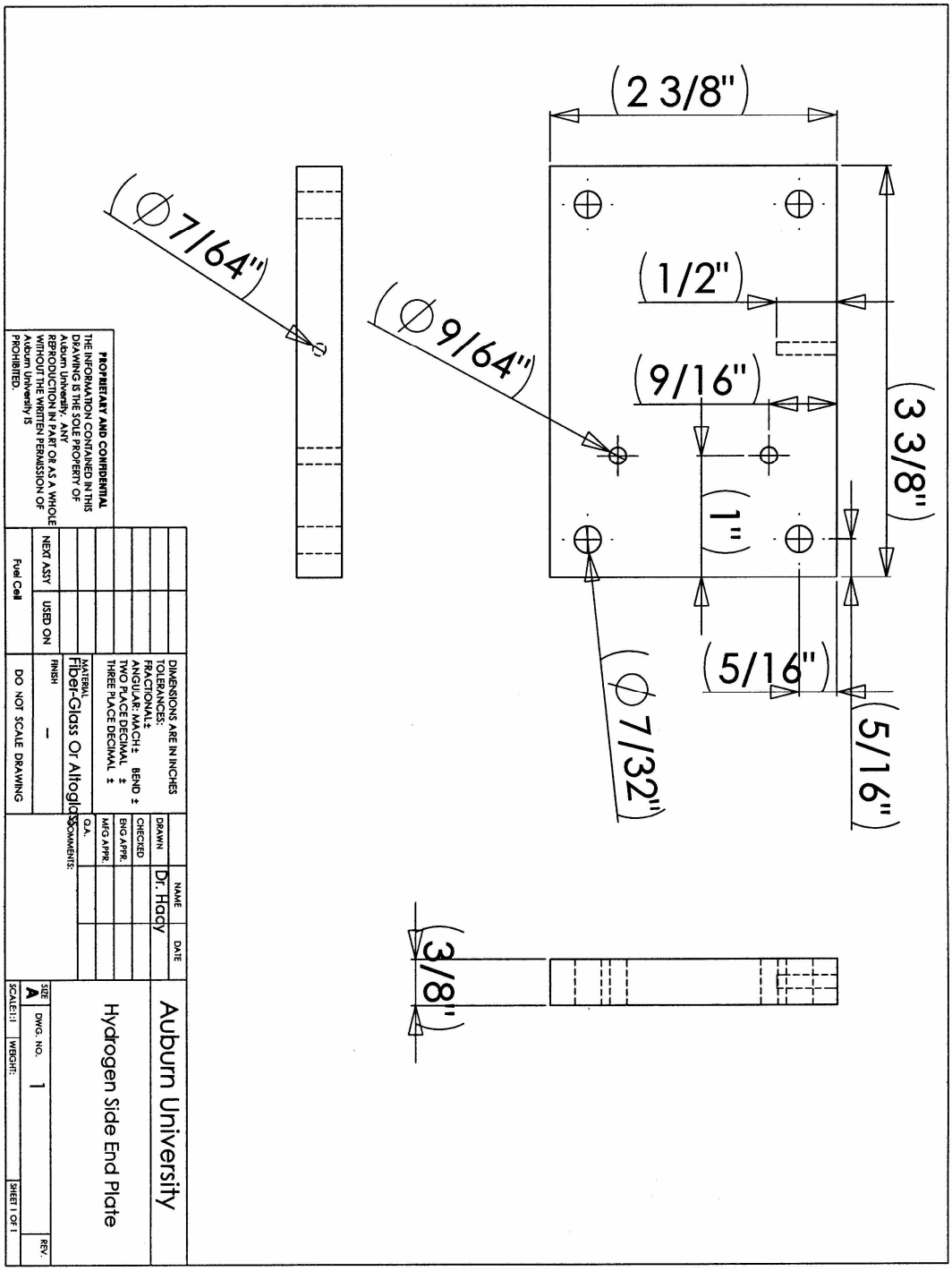

Figure A-3 H_2 side end plate

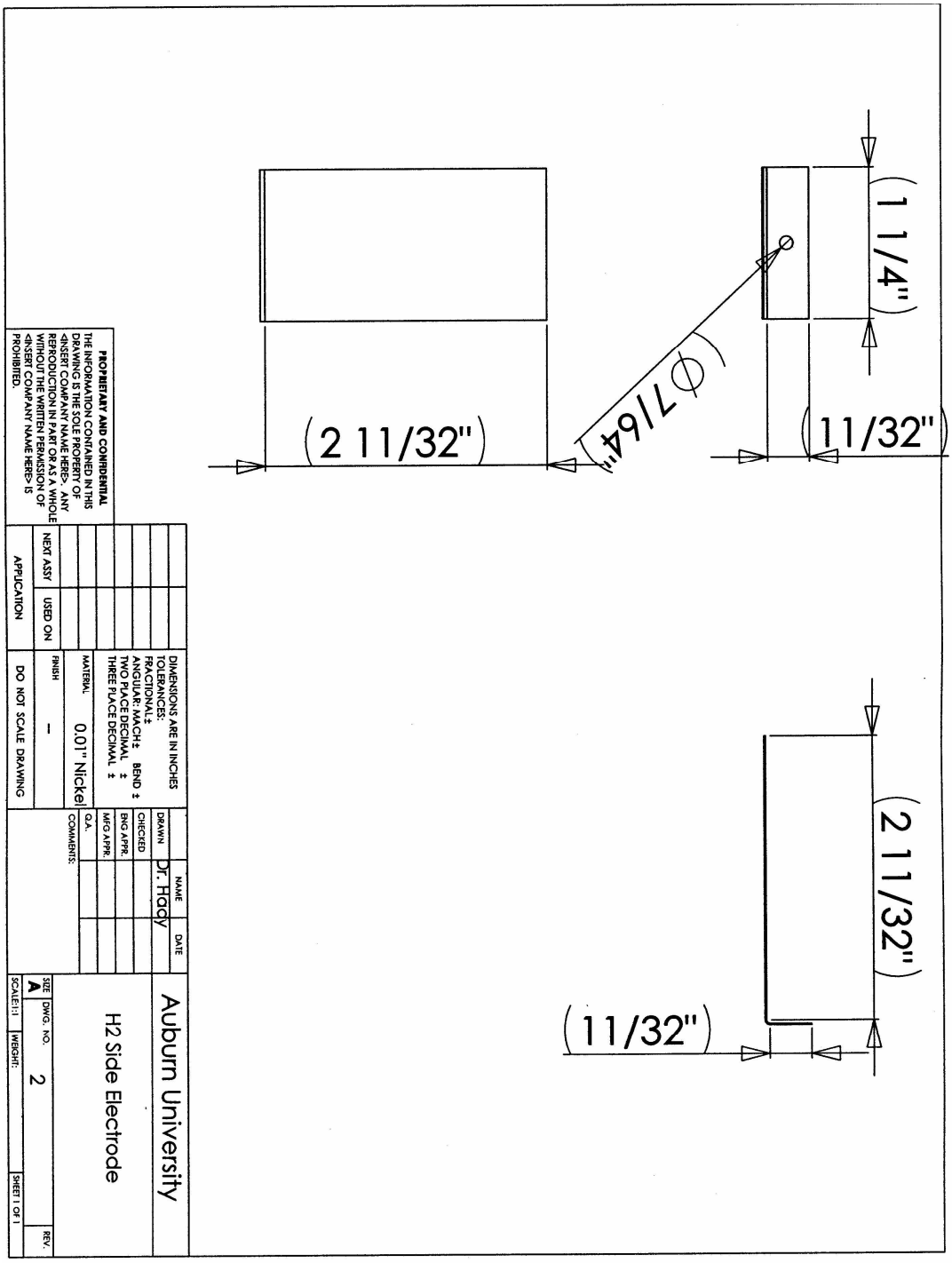

Figure A-4 Hydrogen side electrode

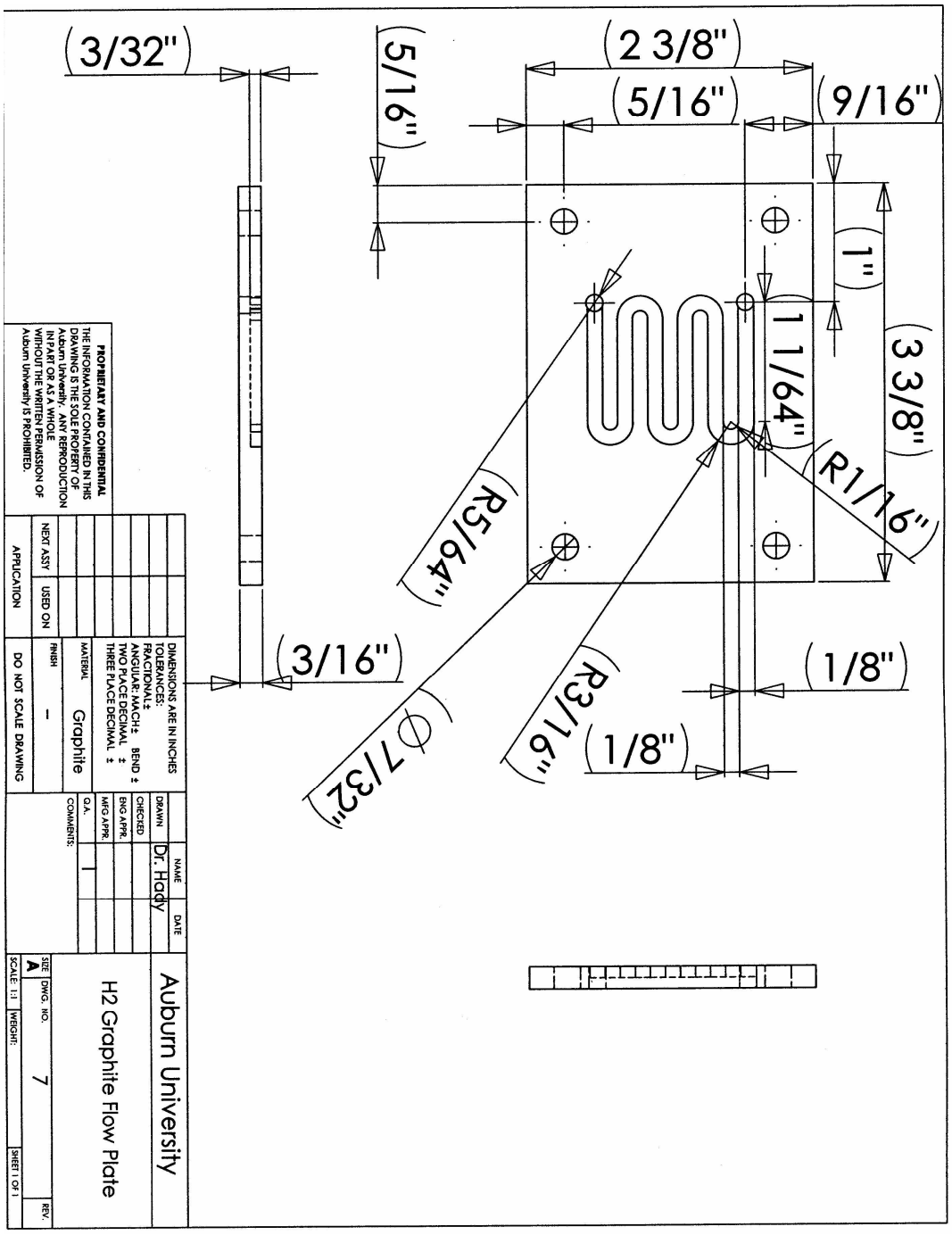

Figure A-5: H_2 graphite flow plate

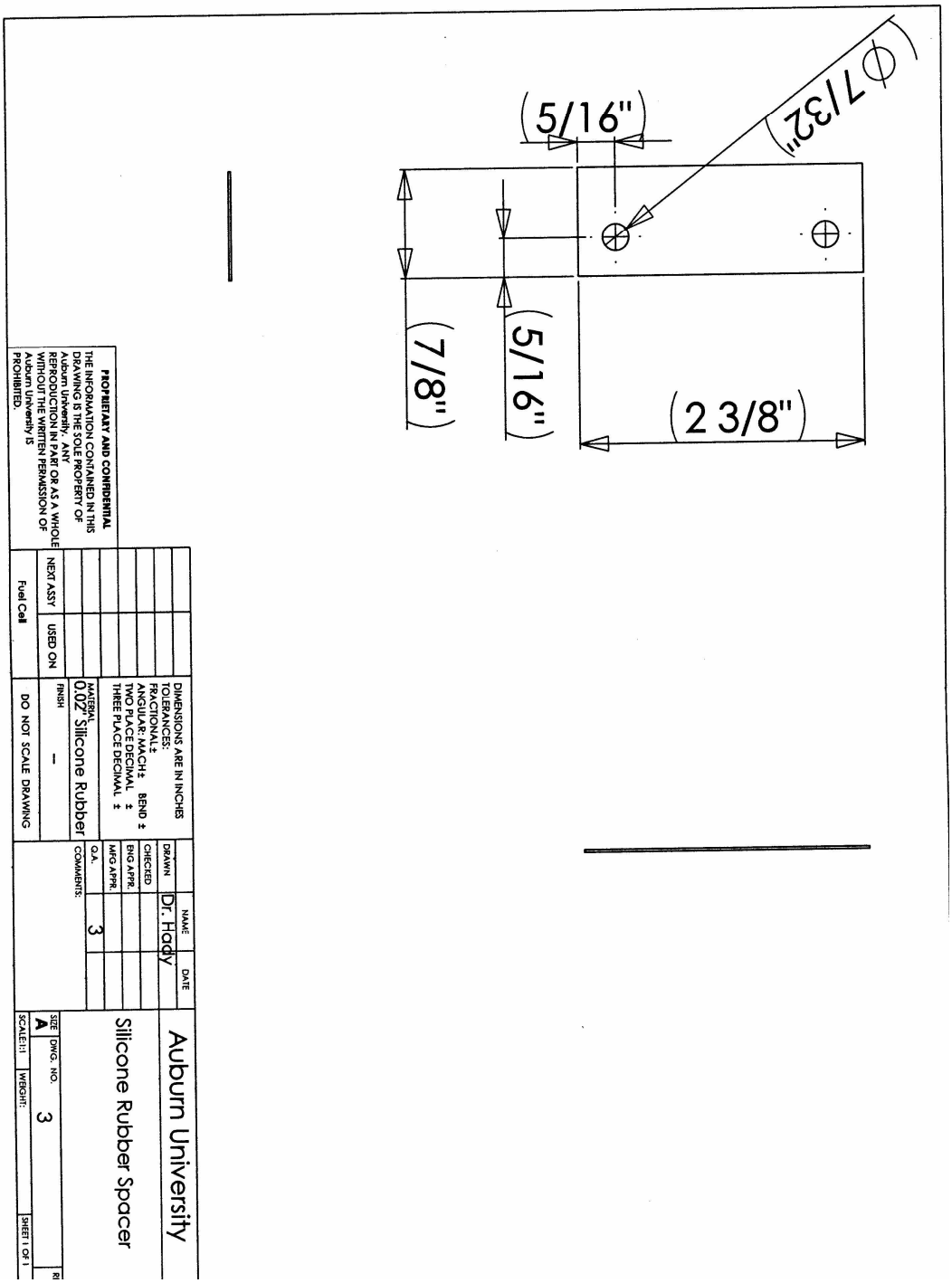

Figure A-6 Silicon rubber spacer

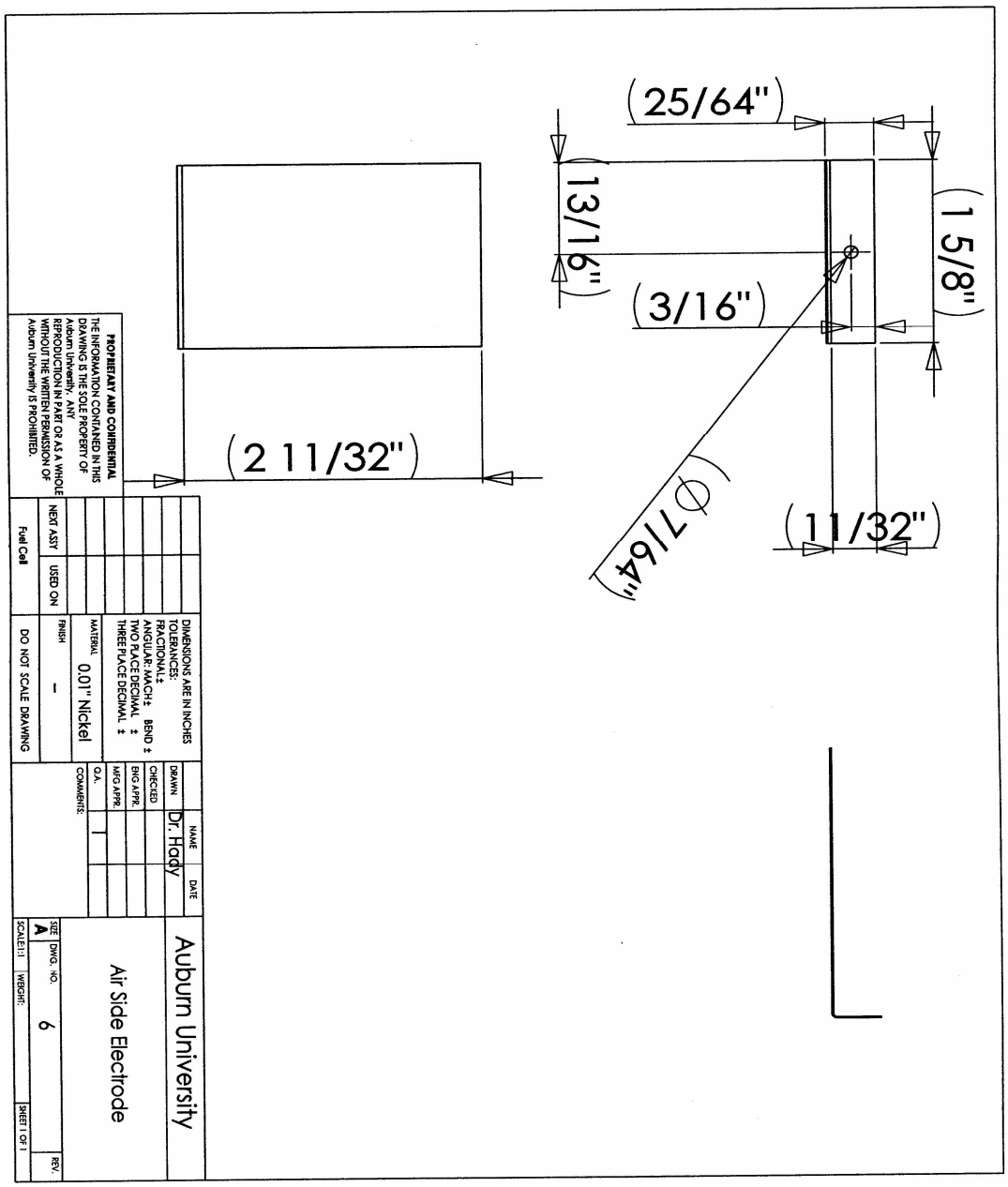

Figure A-7 Air side electrode

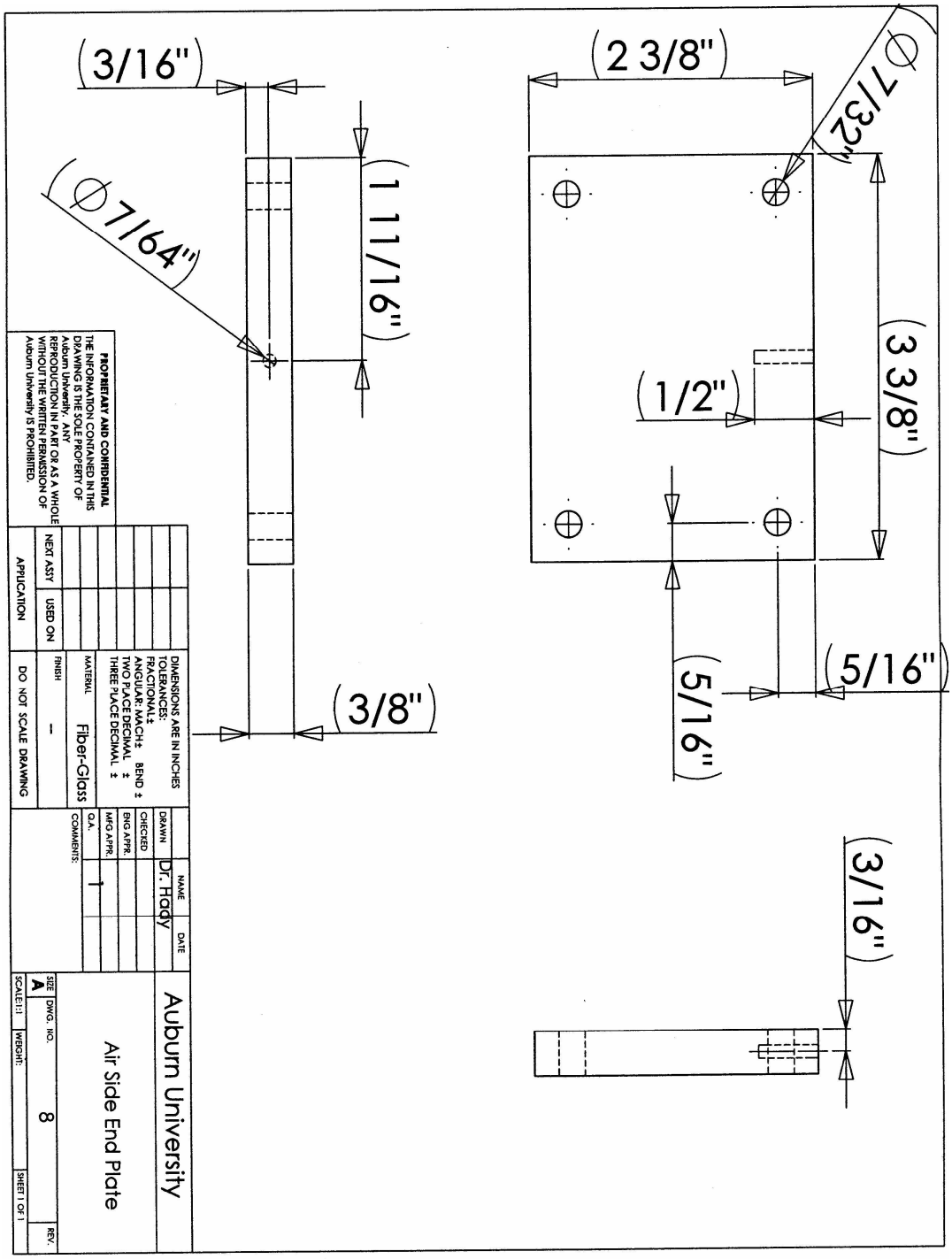

Figure A-8: Air side end plate

APPENDIX B: Photo-Micrographs of The Manufactured Carbon Papers

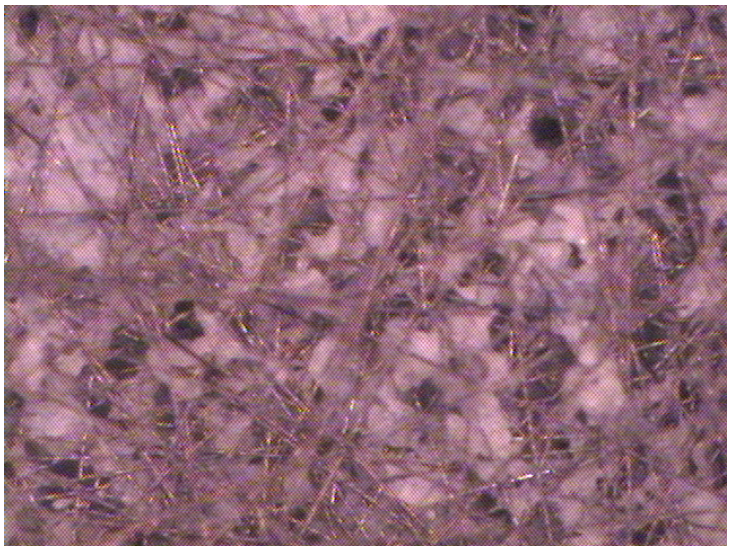

Figure B-1 Sample 15, 63X magnification

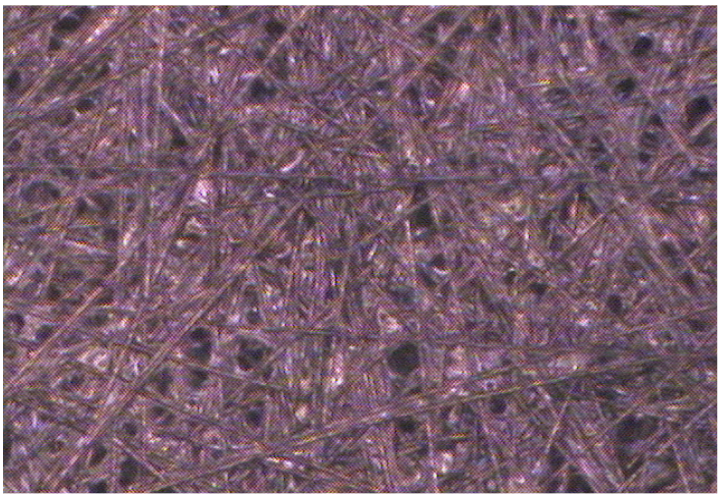

Figure B-2 Sample 13, 90X magnification

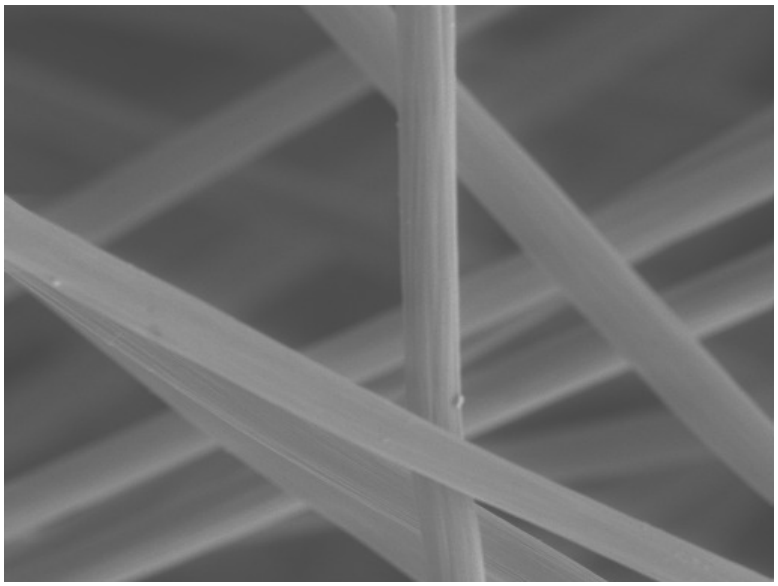

Figure B-3 Sample 1, 1000X magnification

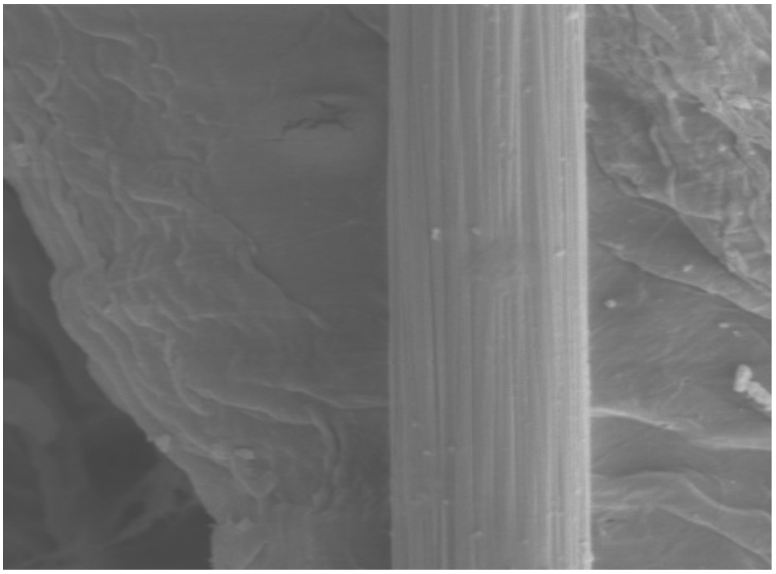

Figure B-4 Sample 4, 5000X magnification

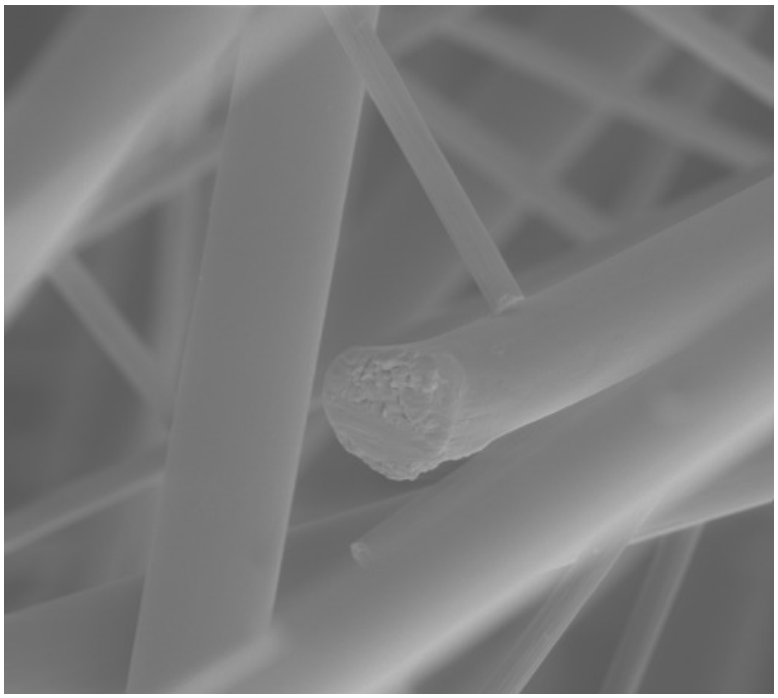

Figure B-5 Sample 5, 500X magnification